Supplementary Information

for

Doxorubicin evicts histones from open chromatin modulating DNA repair and epigenetics for optimal chemotherapy responses

Baoxu Pang[1,7], Xiaohang Qiao[1,7], Lennert Janssen[1], Arno Velds[2], Tom Groothuis[1], Ron Kerkhoven[2], Marja Nieuwland[2], Huib Ovaa[1], Sven Rottenberg[3], Olaf van Tellingen[4], Jeroen Janssen[6], Peter Huijgens[6], Wilbert Zwart[5] and Jacques Neefjes[1]*

[1]Division of Cell Biology

[2]Central Genomic Facility

[3]Division of Molecular Biology

[4]Division of Diagnostic Oncology

[5]Division of Molecular Pathology

The Netherlands Cancer Institute, Plesmanlaan 121, 1066CX, Amsterdam, The Netherlands.

[6]Department of Hematology, VU University Medical Center, Boelelaan 1117, 1081 HV, Amsterdam, The Netherlands.

[7]These authors contributed equally to this work.

*Correspondence: J. Neefjes

Email: J.NEEFJES@NKI.NL

Table of contents:

Supplementary Figures

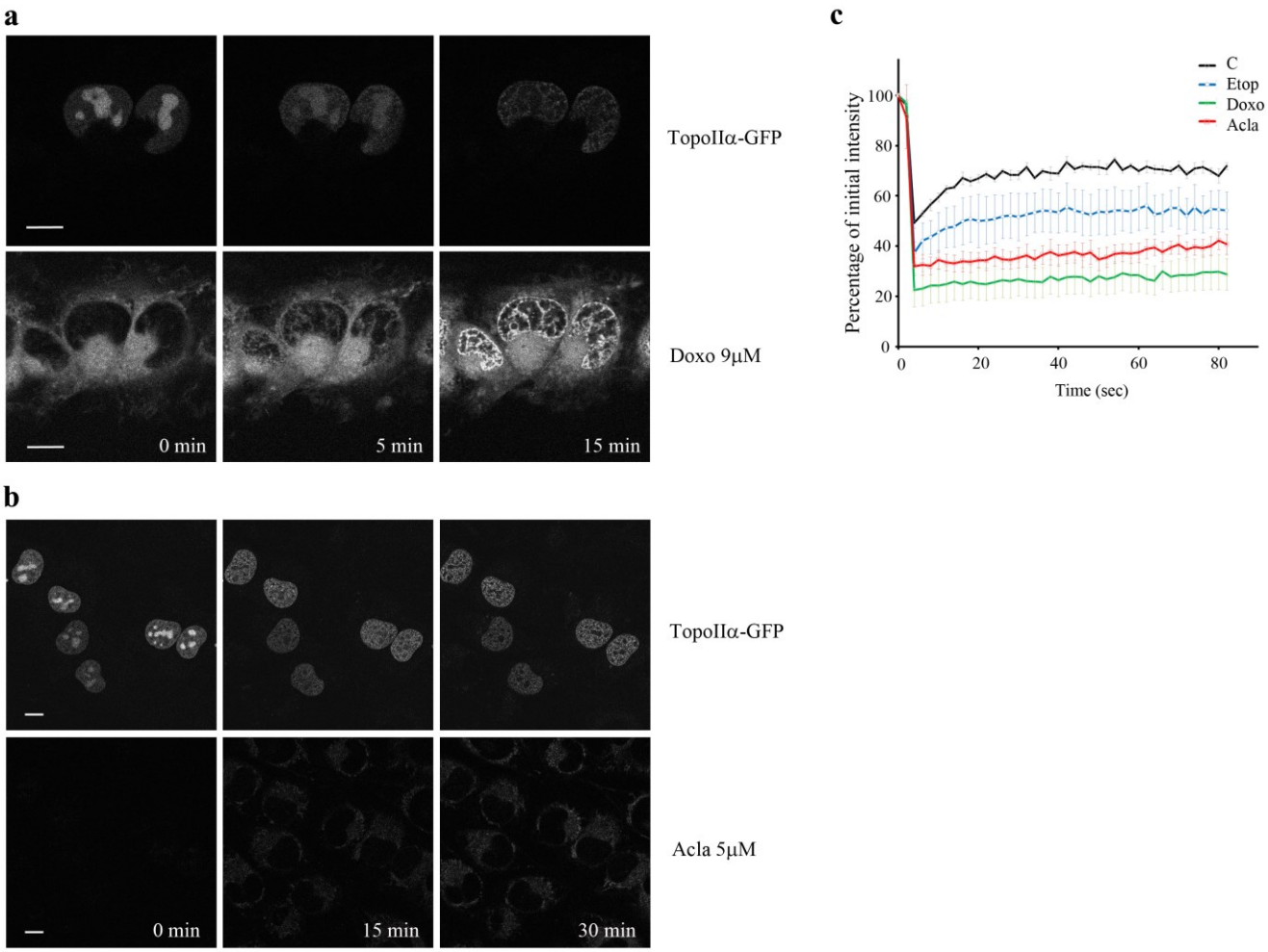

Supplementary Figure S1: Dynamic behavior of TopoIIα in response to the inhibitors used in the study. (**a**) MelJuSo cells expressing TopoIIα-GFP were exposed to 9μM Doxo and the re-localization of TopoIIα-GFP from nucleoli to the chromatin was followed in time (top panel). Bottom panel shows that Doxo (a red fluorophore) enters first the cytosol and after 5 min the nucleus to intercalate into chromatin at sites that acquire TopoIIα-GFP as well. Scale bars, 10μm. Observed in more than 3 independent experiments with full concordance of results. (**b**) MelJuSo cells expressing TopoIIα-GFP were exposed to 5μM Acla and the re-localization of TopoIIα-GFP from nucleoli into chromatin was followed in time (top panel). Unlike Doxo, Acla does not fluorescently label DNA structures (bottom panel). Scale bars, 10μm. Observed in more than 3 independent experiments with full concordance of results. (**c**) MelJuSo cells expressing TopoIIα-GFP were treated for 2 hrs with different drugs as indicated. Then fluorescence recovery after photobleaching (FRAP) experiments on the nuclear pool of TopoIIα-GFP were performed to assay mobility of TopoIIα-GFP under these conditions. Whereas a fraction of TopoIIα-GFP is dynamic in control and Etop-exposed cells (as 20-30% of fluorescent TopoIIα-GFP enters the bleached spot resulting in fluorescence recovery), the two anthracyclines trap most of TopoIIα-GFP (a fluorescence recovery after bleaching in not detected). (n=5 per data point, error bar indicates S.E.M)

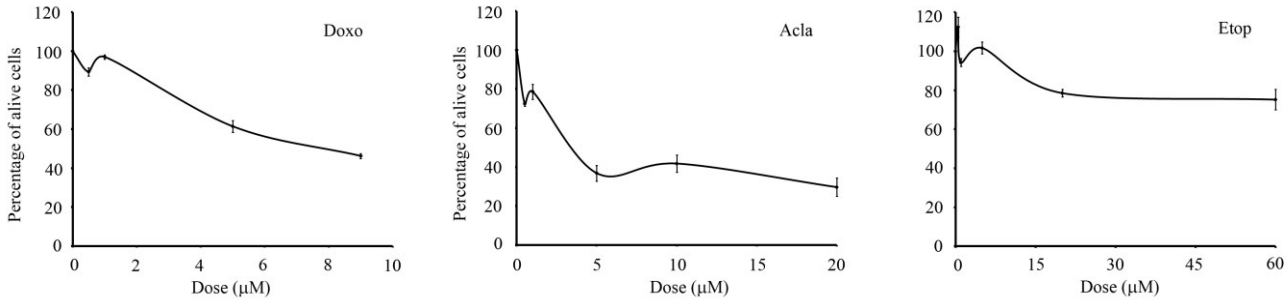

Supplementary Figure S2: Cell viability after 2 hrs exposure to drugs. MelJuSo cells were treated with indicated doses of drugs for 2 hrs. After drug removal by extensive washing, cells were further cultured for another 24 hrs and cell viability was measured using CellTiter Blue assay. The anthracyclines are more toxic than Etop. (n=3, error bar indicates S.E.M.)

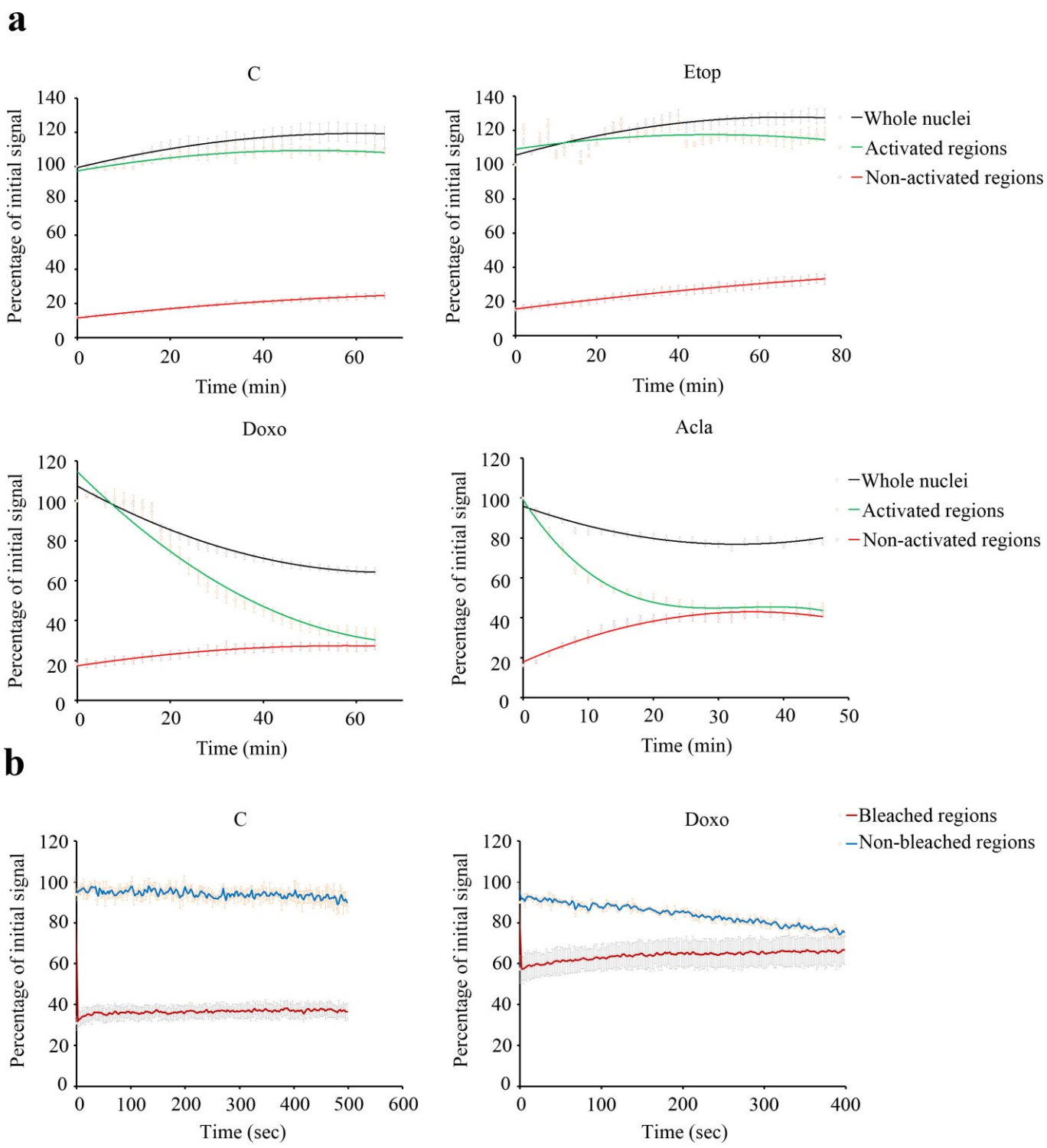

Supplementary Figure S3: ***Dynamics of different histones in response to doxorubicin and aclarubicin (relates to Figure 1b).*** (**a**) Fluorescence intensity of cells treated with respective drugs in Figure 1b was quantified and the average intensity of the activated regions, non-activated regions and whole nuclear regions were plotted. (n=6 to 8 cells per data point, error bar indicates S.E.M.). Loss of fluorescence in the photoactivated region following Doxo or Acla exposure is not the result of bleaching, as the total fluorescence in the nucleus is only marginally affected. Note the converging of the signal from activated and non-activated regions, indicating release of histones from the activated areas and entry in the non-activated ones. Since histones are released into 3D volume of the nuclei, the decrease of the total fluorescence in the confocal plane could be the result of the diffusion of evicted histones. To test whether Doxo has an additional effect on histone H2A degradation unlike Acla, we quantified the total fluorescence of GFP-labeled histones at various time points. We did not observe fluorescence loss in Doxo treated H2B-GFP cells, unlike Doxo treated H3/H4-GFP cells (Supplementary Figure 3e), when total fluorescence was quantified in a time-lapse mode with high content imaging. (**b**) After 2 hrs drug exposure, FRAP experiments were performed on cells as in Figure 1b, to confirm the mobility of released histones in Doxo-treated cells. Fluorescence intensities were quantified at the bleached regions and the non-bleached regions within the same cells. (for each data point n=3, error bar indicates S.E.M.)

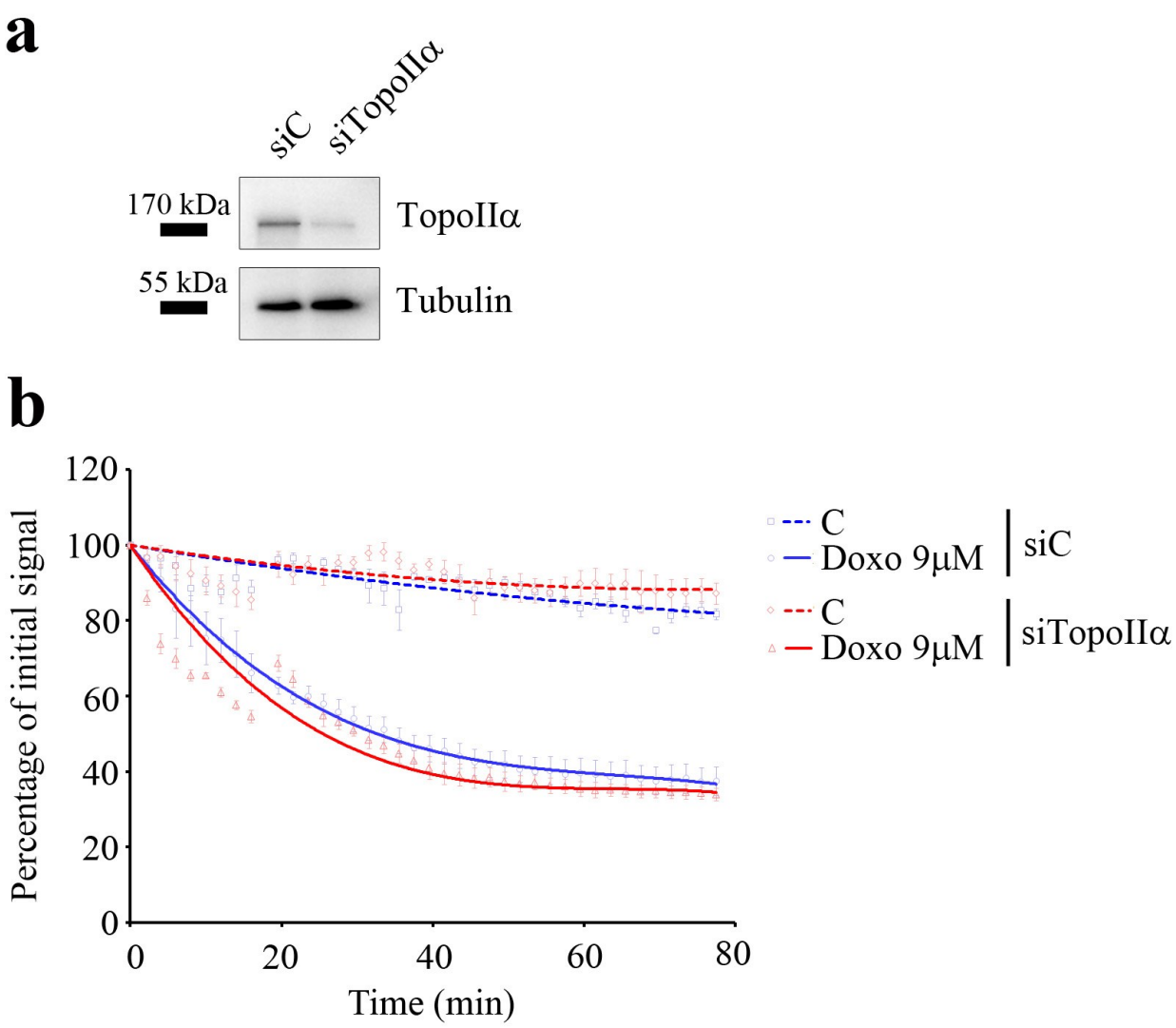

Supplementary Figure S4: TopoIIα levels do not correlate to doxorubicin-induced histone eviction. (**a**) MelJuSo/PAGFP-H2A cells were transfected with pools of DharmaFECT siRNA against TopoIIα or scrambled control. 72 hrs after siRNA transfection, lysates of cells were prepared and separated by SDS-PAGE followed by WB and probing for TopoIIα and tubulin as loading control. Positions of marker proteins are indicated. (**b**) Small regions in the nucleus of TopoIIα knockdown or control MelJuSo/PAGFP-H2A cells were photoactivated with 405nm laser light, and the histone diffusion was monitored in the presence or absence of 9μM Doxo (as in Figure 1b). Silencing TopoIIα does not affect Doxo-induced histone eviction. (n=5 per data point, error bar indicates S.E.M).

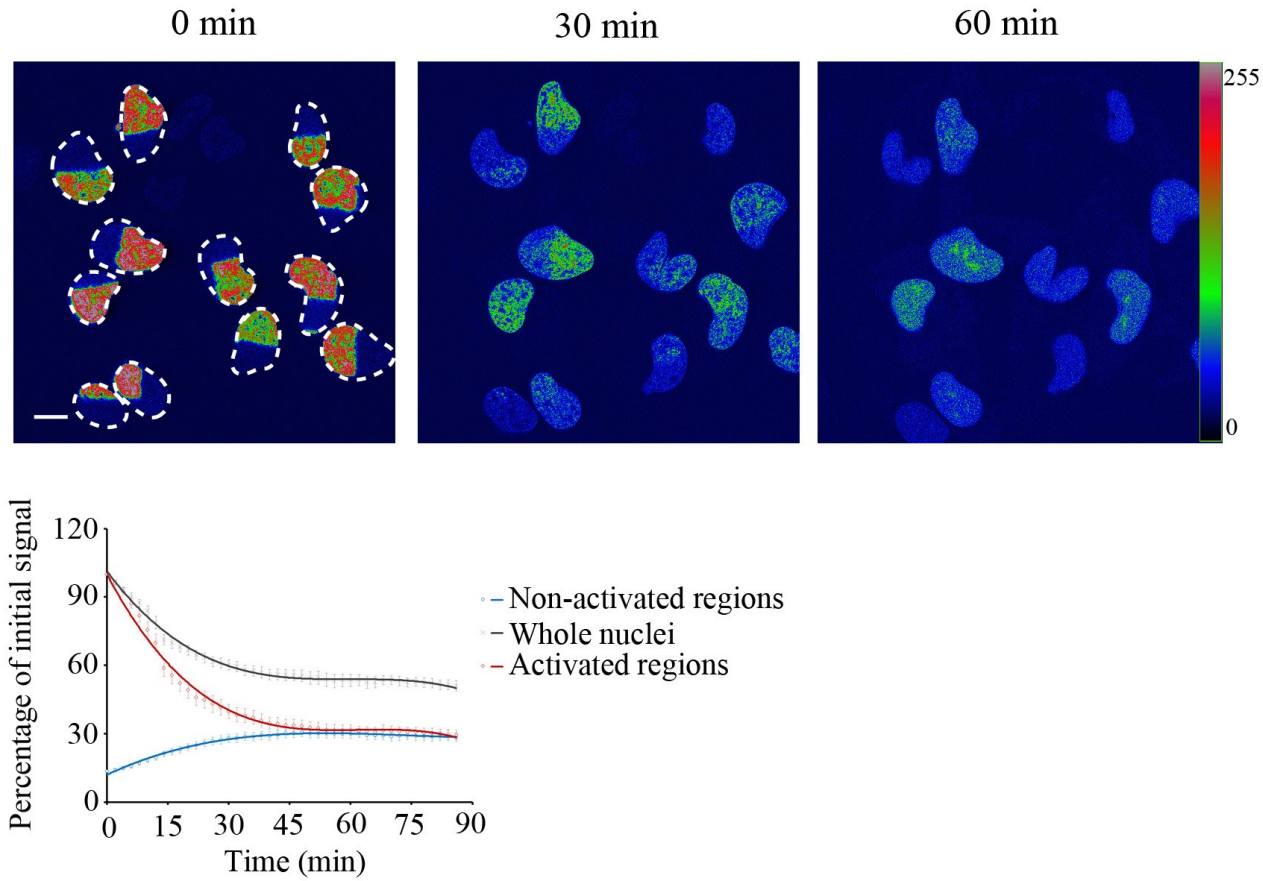

Supplementary Figure S5: ***Doxorubicin-induced histone eviction is not due to apoptosis (relates to Figure 1b).*** MelJuSo cells expressing PAGFP-H2A were pre-treated with 50μM pan-caspase inhibitor Z-VAD for 2 hrs to block the initiation of apoptosis. Then part of the nucleus was photoactivated with 405nm laser light. The cells were exposed to 9μM Doxo for the times indicated and the fate of PAGFP-H2A was monitored by CLSM. The boundaries of nuclei are indicated. The fluorescence intensities are shown in false colors as indicated by the 'Look-Up Table'. Scale bar, 10μm. Fluorescence intensities were quantified at the activated regions, non-activated regions and whole nuclear regions within the same cells. Caspase inhibition did not affect Doxo-induced histone eviction. (n=7 per data point, error bar indicates S.E.M).

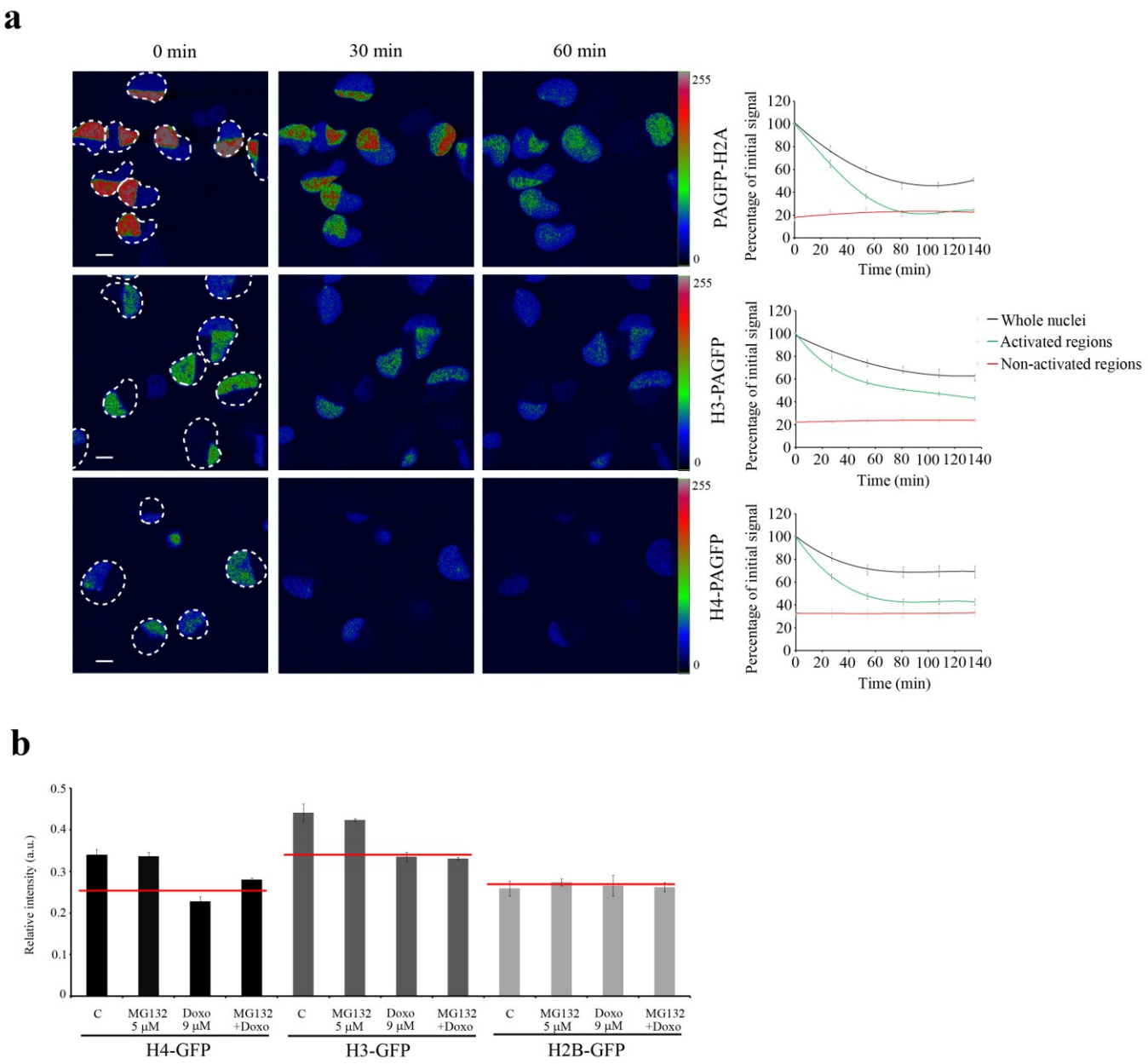

Supplementary Figure S6: ***Histone variants have different fates after doxorubicin-induced eviction (relates to Figure 1b).*** (**a**) About half of the nucleus from MelJuSo cells stably expressing PAGFP-labeled histone H2A (top panel), H3 (middle panel) or H4 (lower panel) was photo-activated with 405nm laser light. The cells were subsequently exposed to 9µM Doxo and imaged by CLSM at indicated time points. Look-Up Table shows the relative intensities of fluorescence. The boundaries of nuclei are indicated. The photoactivated areas are visible at the start of the experiment (0 min time point). Scale bar, 10µm. Right panels: fluorescence intensities were quantified at the activated regions, non-activated regions and whole nuclear regions within the same cells as indicated. No increase in fluorescence in the non-activated regions from H3/H4-PAGFP expressing MelJuSo cells was observed, probably due to fast degradation. (n=4 to 5 per data point, error bar indicates S.E.M.). (**b**) MelJuSo cells stably expressing GFP-labeled histone variants H3, H4 or H2B were treated with indicated drugs for 4 hrs. The proteasome inhibitor MG132 was included to test a possible contribution of proteasomal degradation in histone release. Then cells were fixed and imaged using a BD Pathway high-content bioimager for high content low resolution quantification. Average intensity of cells in each treatment was calculated with CellProfiler software[61] (on average 2900 cells per triplicate well per treatment). Total H2B-GFP was not affected by Doxo and MG132 treatment, while Doxo treatment reduced H3-GFP and H4-GFP intensities by some 20% irrespective of proteasome inhibition. Note that proteasome inhibitor MG132 did not prevent the degradation of evicted H3/H4-GFP, as also observed by others[62]. This suggests that proteases different from the proteasome mediate degradation of free histones.

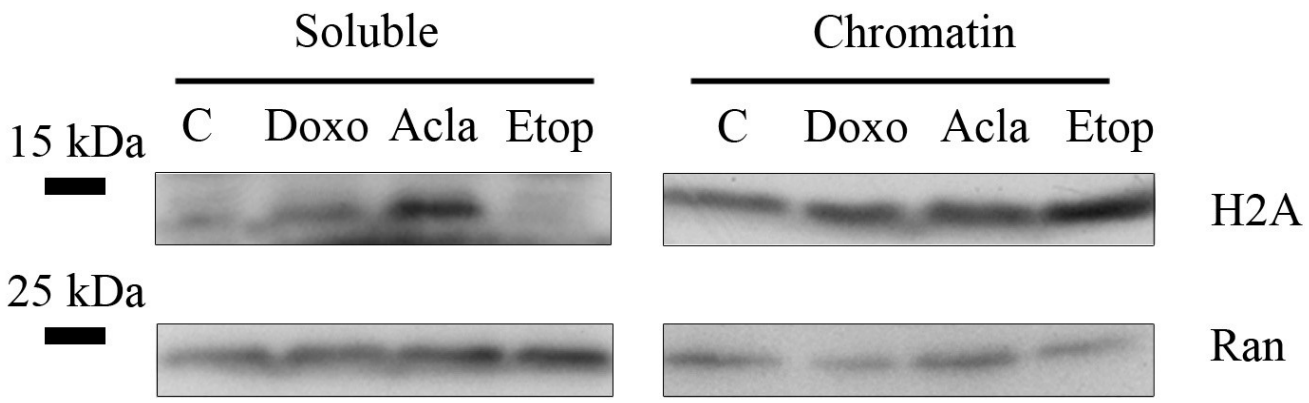

Supplementary Figure S7: Release of endogenous histone H2A by TopoII inhibitors. MelJuSo cells were exposed to 9μM Doxo, 20μM Acla or 60μM Etop for 4 hrs. Chromatin was separated from the soluble fraction of the cells. The soluble and chromatin fractions were separated by SDS-PAGE and H2A was detected by WB. Ran GTPase was used as the loading control.

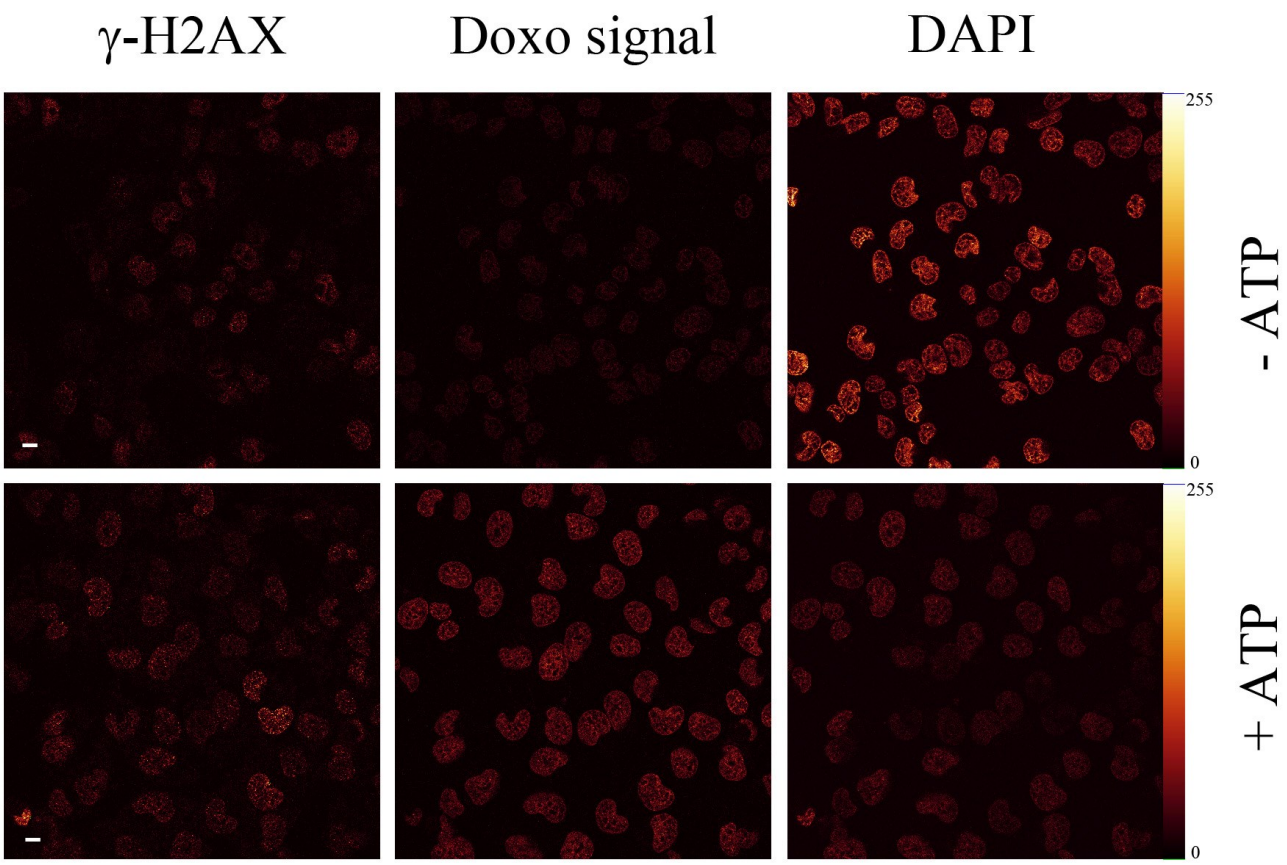

Supplementary Figure S8: ATP dependent processes are involved in doxorubicin uptake into cells. ATP was depleted in MelJuSo cells by NaAz and 2-deoxyglucose treatment[63]. Then control or ATP-depleted cells were exposed to 9μM Doxo for 2 hrs before fixation. Cells were also stained for γ-H2AX. Images were taken under identical settings. DAPI visualizes the position of the nuclei. Because Doxo also competes for the intercalation sites with DAPI, DAPI staining was lower in cells where Doxo accumulated. Doxo accumulation was significantly impaired during ATP depletion. Intensities are shown in the glow-over/under mode. Scale bar, 10μm.

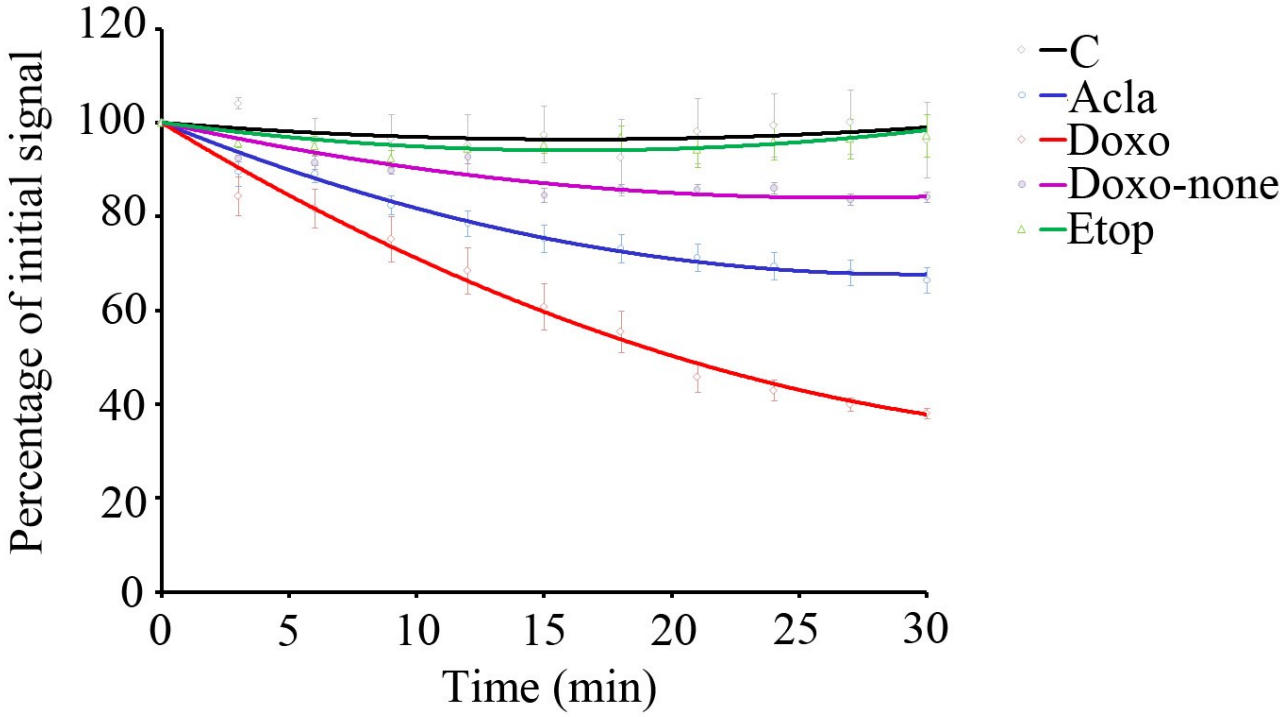

Supplementary Figure S9: Quantification of PAGFP-H2A fluorescence intensities in Triton-permeabilized cells exposed to different drugs (relates to Figure 2a). MelJuSo cells expressing PAGFP-H2A were permeabilized with Triton X-100 prior to photoactivation of PAGFP-H2A with 405nm laser light. The nuclei were subsequently exposed to 9µM Doxo, 20µM Acla, or 60µM Etop and the fluorescent signal was followed over time by CLSM. Histones are released by Doxo and Acla but not by Etop and Doxo-none. Images are taken at the indicated time points and the fluorescence was quantified. Shown are trend lines that connect the mean fluorescence data (n=10 to 20 cells per time point, error bar indicates SEM). The respective drug treatments (in different colors) are indicated.

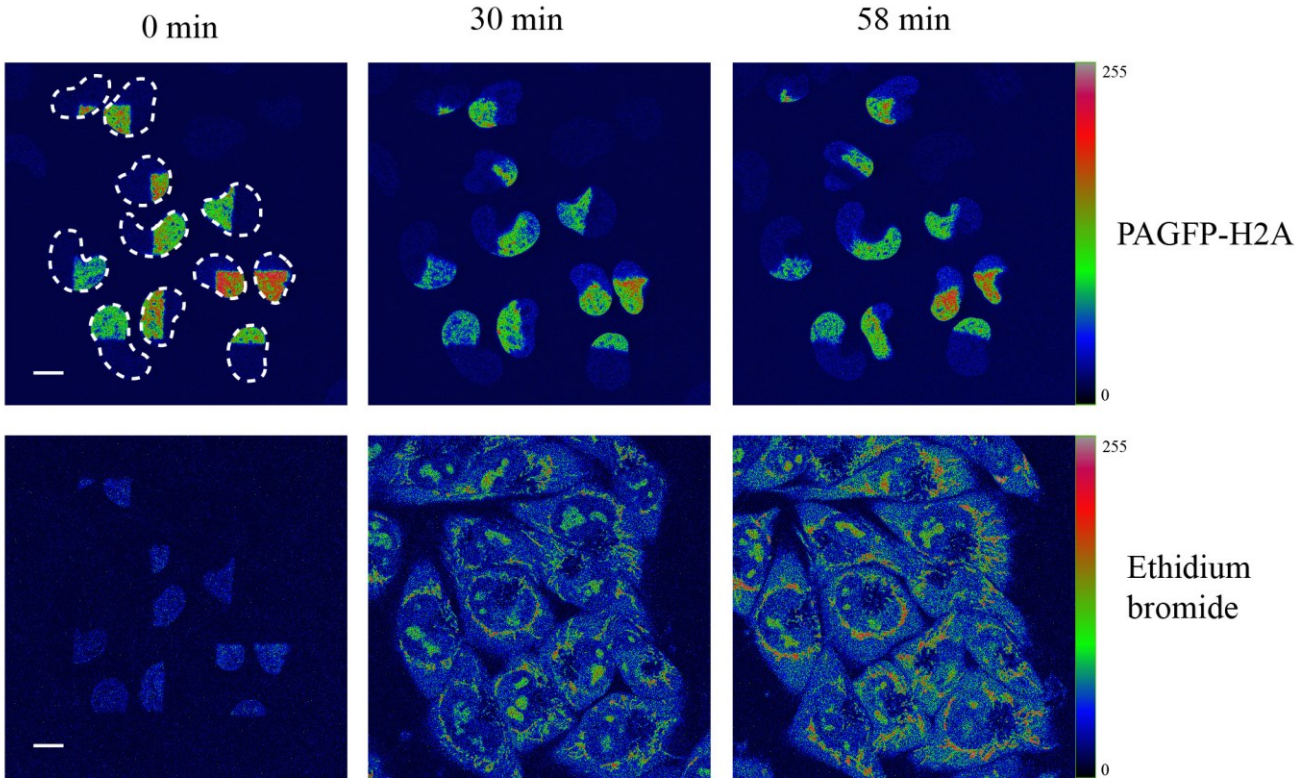

Supplementary Figure S10: The DNA intercalator Ethidium-Bromide does not evict histones. Half the nucleus of MelJuSo cells expressing PAGFP-H2A was photo-activated by 405nm laser light (upper panel). Then cells were exposed to 10µg/ml ethidium bromide (detected by 488nm laser light, lower panel) and cultured for the times indicated while imaged by CLSM, as in Figure 1b. This indicates that histone eviction is not induced by each DNA intercalating agent but has selectivity for the anthracyclines Doxo and Acla. The positions of the nuclei are indicated in the top-left figure. Scale bar, 10µm.

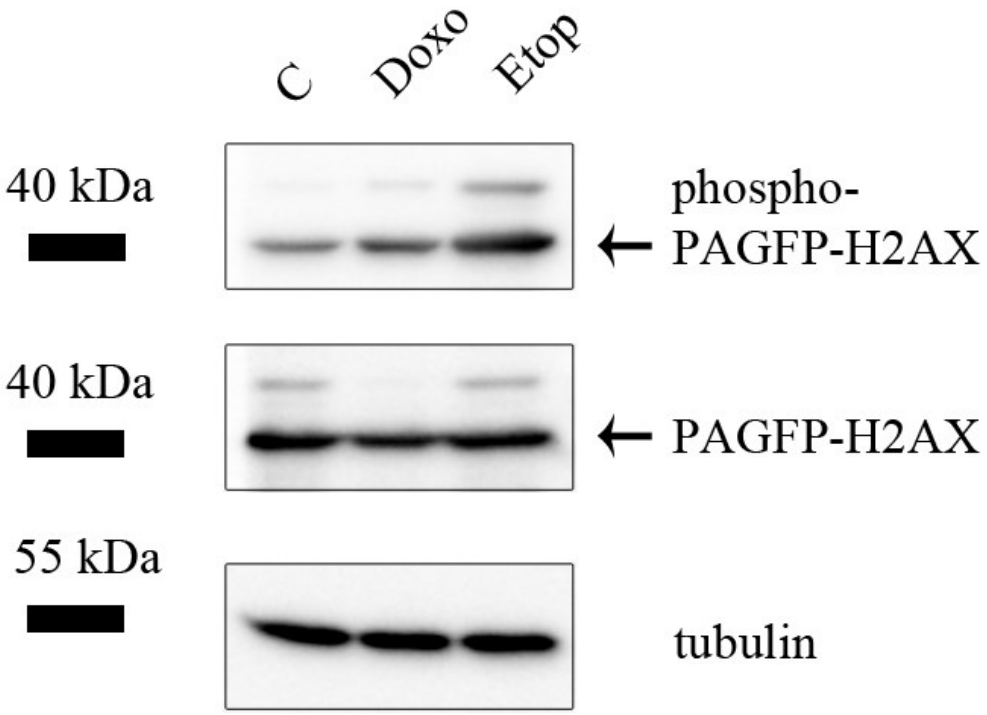

Supplementary Figure S11: PAGFP-labeled H2AX can be phosphorylated following DNA damage. MelJuSo cells stably expressing PAGFP-H2AX were cultured in the presence of either 9μM Doxo or 60μM Etop for 2 hrs. Cells without treatment are indicated as C. The cells were lysed, analyzed by SDS-PAGE and Western blotting. Equal amounts of total protein were loaded and the filter was probed with anti-γ-H2AX and GFP. β-tubulin was used as a loading control.

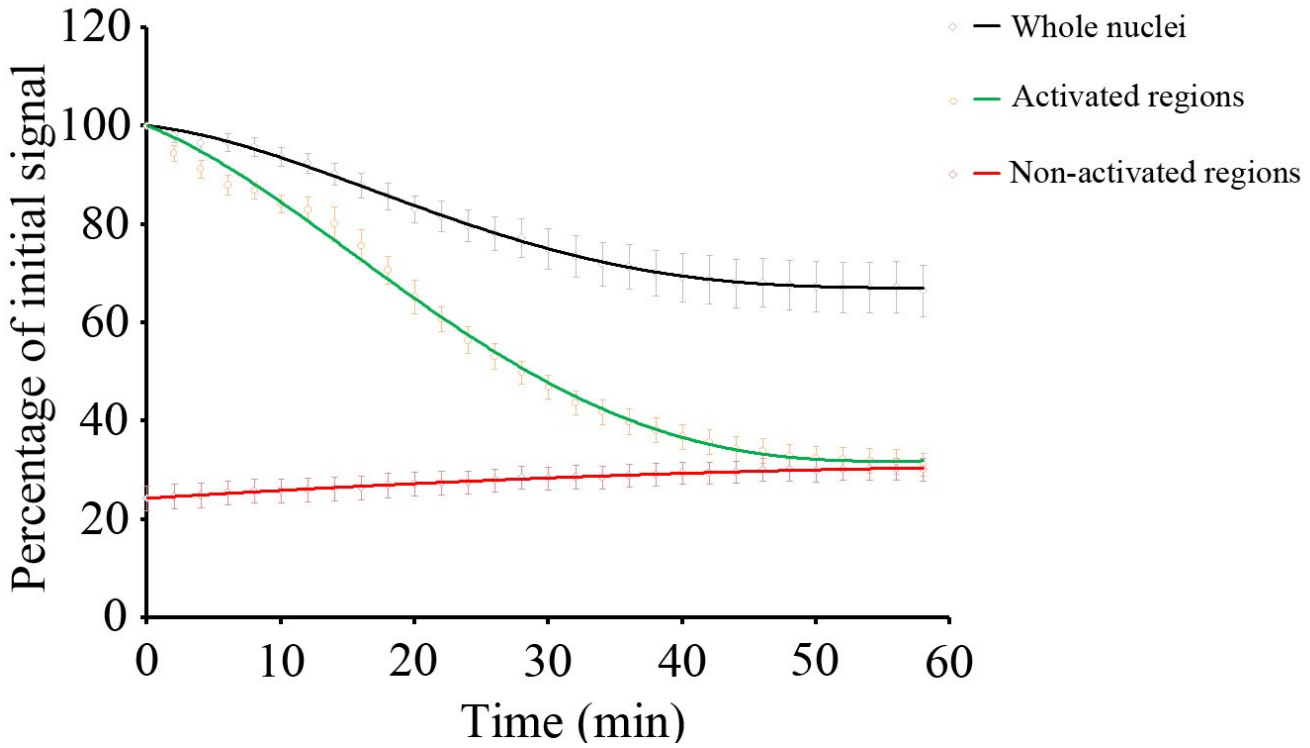

Supplementary Figure S12: Quantification of PAGFP-H2AX release during doxorubicin treatment. Fluorescence intensities of MelJuSo cells stably expressing PAGFP-H2AX in Figure 3a were quantified and the average intensities of the activated regions, non-activated regions and total nuclear regions were plotted. (n=9 cells per data point, error bar indicates S.E.M.). Fluorescence redistribution of PAGFP-H2AX was identical to that of PAGFP-H2A.

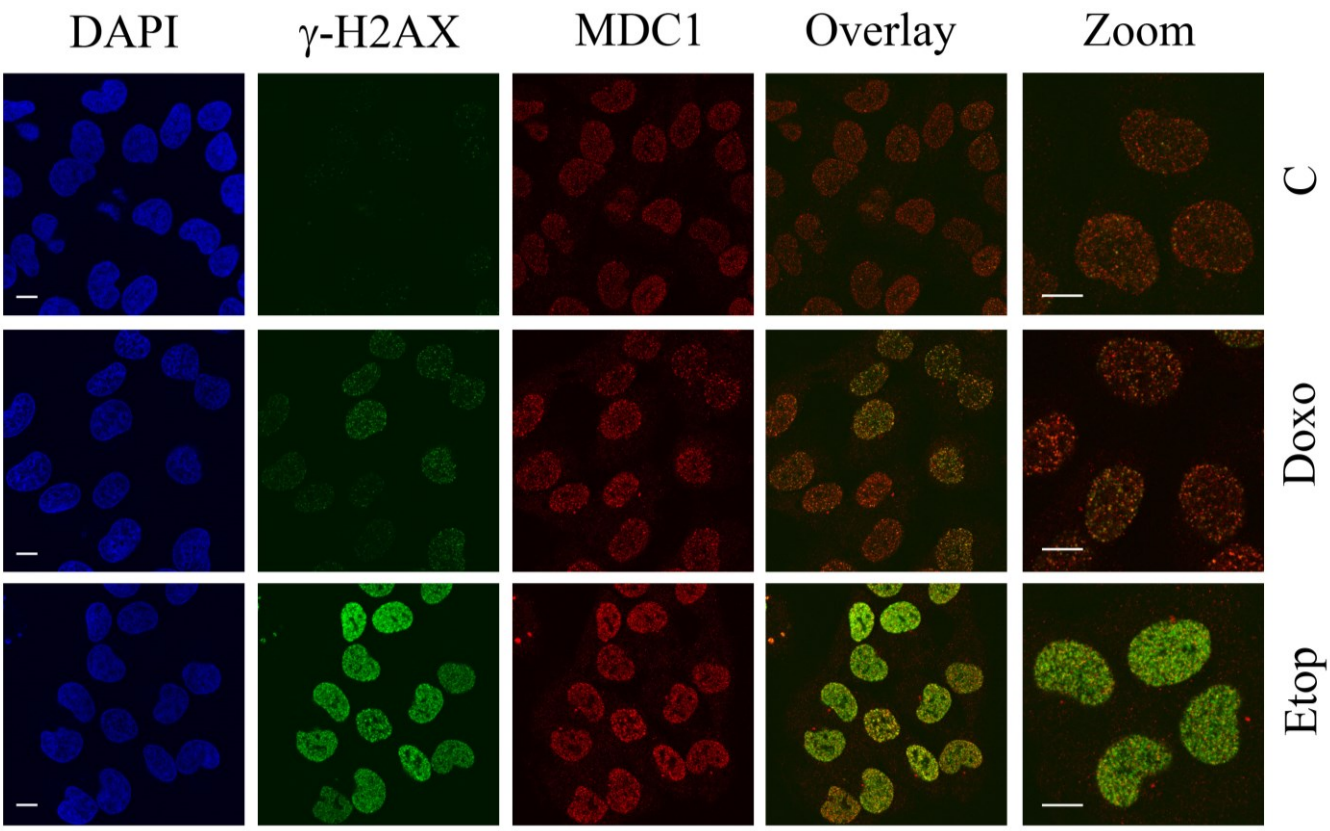

Supplementary Figure S13: The effect of doxorubicin or etoposide on various components of the DNA Damage Repair Response. MelJuSo cells were cultured in the presence or absence (C) of either 9μM Doxo or 60μM Etop for 2 hrs. Then cells were fixed and co-stained for γ-H2AX and MDC1 before analyses by CLSM under identical settings. As the immediate downstream factor which directly binds to γ-H2AX, MDC1 co-localized with γ-H2AX in both Doxo and Etop treated cells. But the staining was lower in Doxo-treated cells. This indicates that the DDR response was interrupted at the level of H2AX phosphorylation. Scale bar, 10μm.

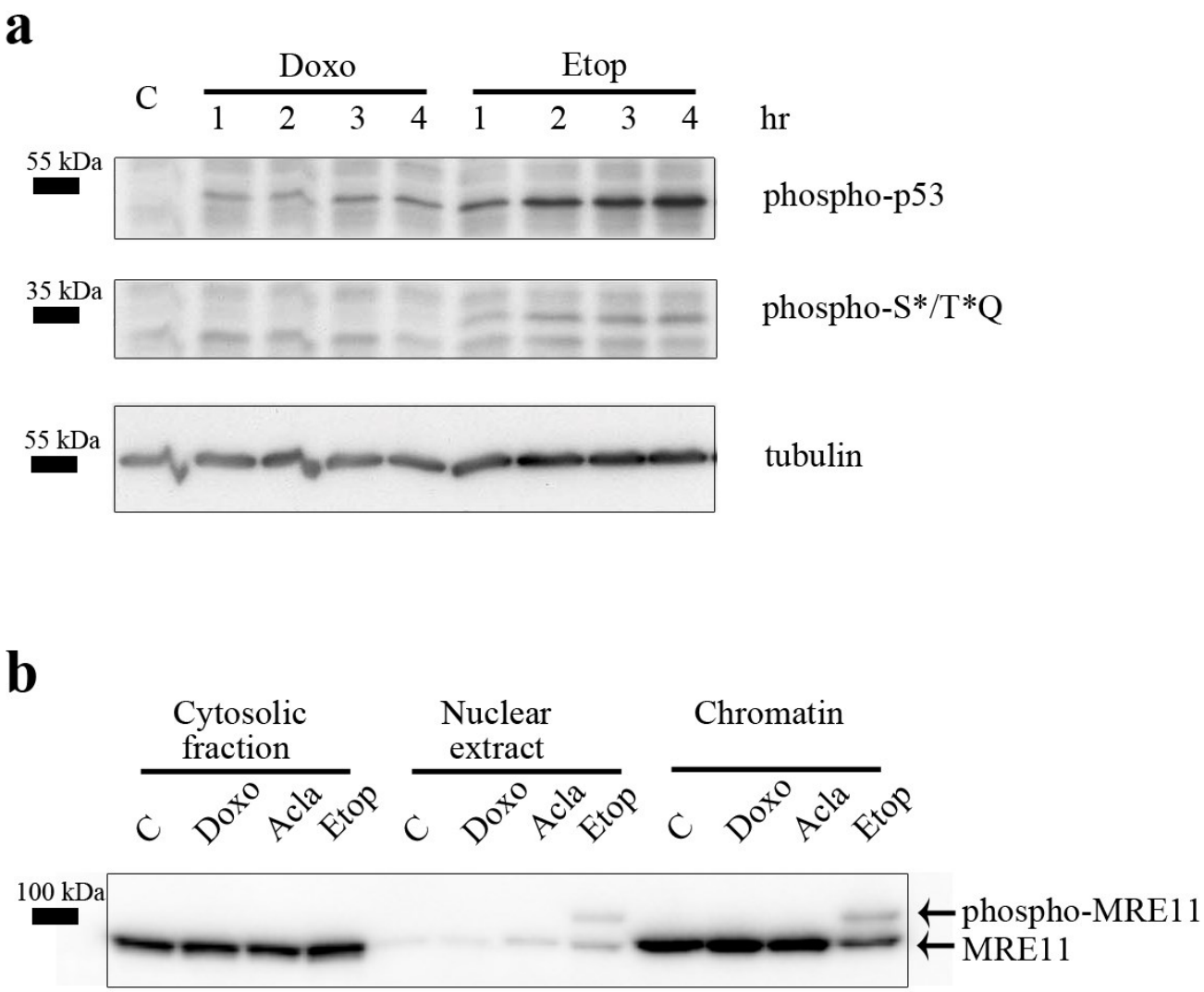

Supplementary Figure S14: Doxorubicin attenuates DNA damage responses. (**a**) MelJuSo cells were exposed to 9μM Doxo or 60μM Etop and were lysed at the indicated time points post-drug exposure, as in Figure 3c. Lysates were separated by SDS-PAGE and analyzed by Western Blotting. The filters were probed with antibodies against phospho-p53 and phospho-S*/T*Q (phospho-(Ser/Thr) substrates of ATM/ATR). β-tubulin was detected as a loading control. Positions of marker proteins are indicated. (**b**) MelJuSo cells were treated with 9μM Doxo, 20μM Acla or 60μM Etop for 4 hrs. Then cells were fractionated and equal amounts of total protein (as determined by the BioRad Bradford assay) from the nuclear, cytosolic and chromatin fraction of the respective treatments were analyzed by SDS-PAGE and Western Blotting. The filter was probed with anti-MRE11 antibodies detecting the major component of MRN complex that recognize the DNA double-strand breaks. Slower migrating bands represent the phosphorylated form of MRE11, which was only observed following Etop treatment. The positions of molecular weight markers are indicated.

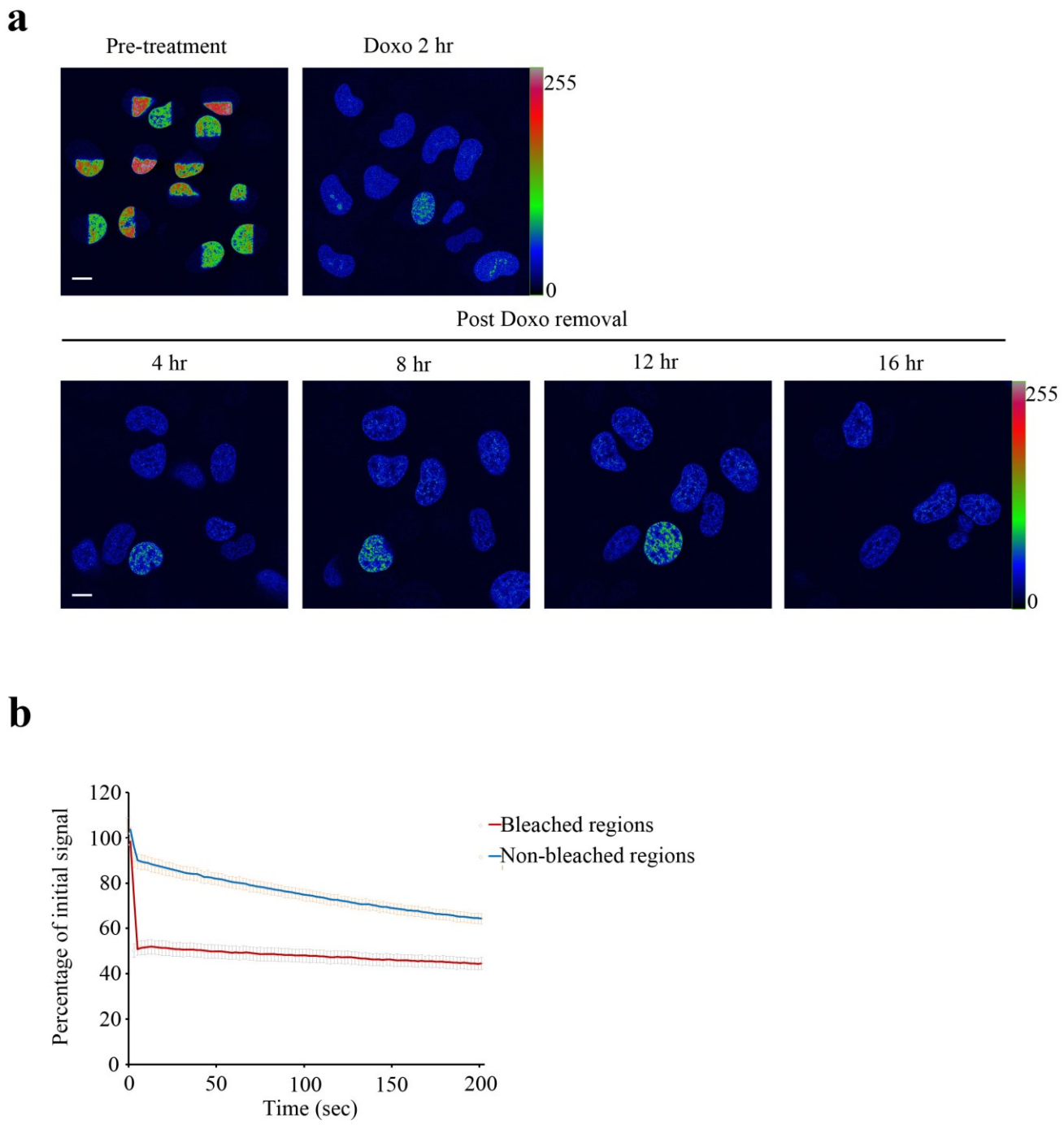

Supplementary Figure S15: Re-entry of doxorubicin-evicted histones into chromatin. (**a**) Half of the nucleus of MelJuSo cells expressing PAGFP-H2A was photo-activated by 405nm laser-light before exposure to 9μM Doxo for 2 hrs, during which histones were released and redistributed in the nucleoplasm. Doxo was removed by washing followed by culturing the cells at 37ºC and analyses by CLSM at the time points indicated. Shown are snapshots of the identical area in time-lapse. While photoactivated PAGFP-H2A initially covered the full nucleoplasm after Doxo exposure, at later time points the typical structure of chromatin in cells was restored with other areas devoid of fluorescence. The fluorescence intensities are shown in false colors as indicated by the "Look-Up Table". Scale bar, 10μm. (**b**) 16 hrs post drug removal, FRAP experiments were performed on MelJuSo cells expressing PAGFP-H2A treated as in Supplementary Figure 13a. The flouresecent histone pool has initially been photoactivated by 405nm light, as in other experiments. To determine whether the evicted fluorescent PAGFP-H2A pool was stably (as indicated by an immobile fraction) re-incorporated into chromatin, FRAP experiments were performed in the nuclear area originally positioned outside the photoactivated half of the nucleus to ensure that the fluorescent pool arrived there by diffusion from the photoactivated half of the nucleus. No recovery of fluorescence in the bleached area was observed indicating stable re-incorporation of fluorescent PAGFP-H2A. (n=9 cells per data point, shown is mean +/- S.E.M)

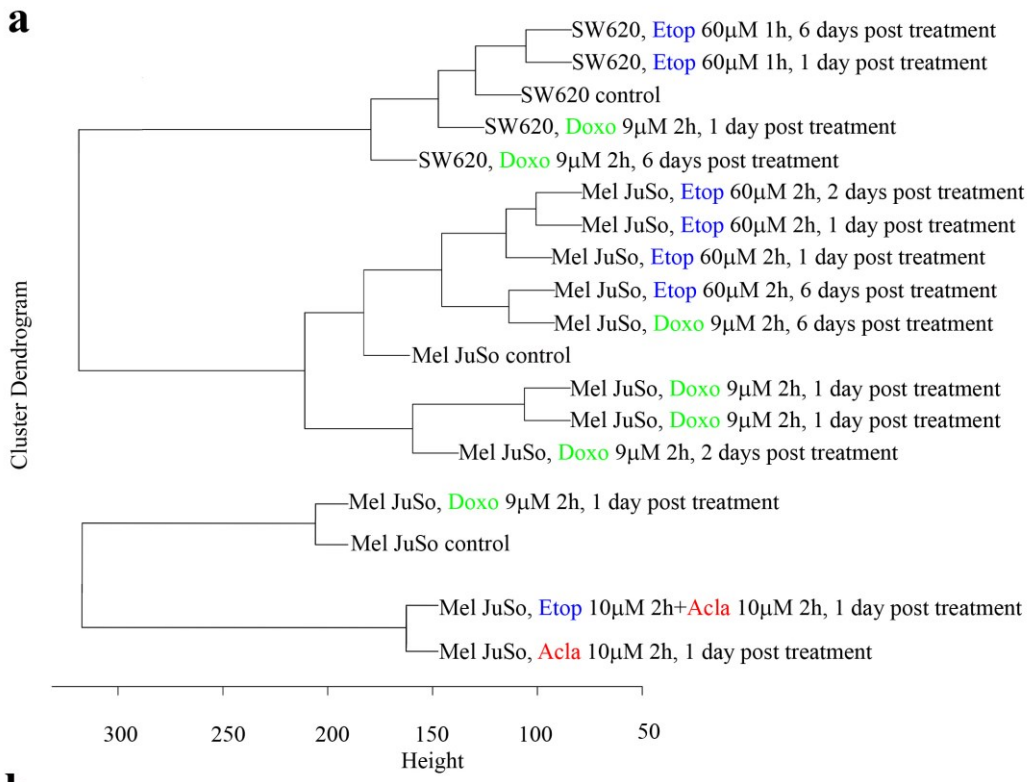

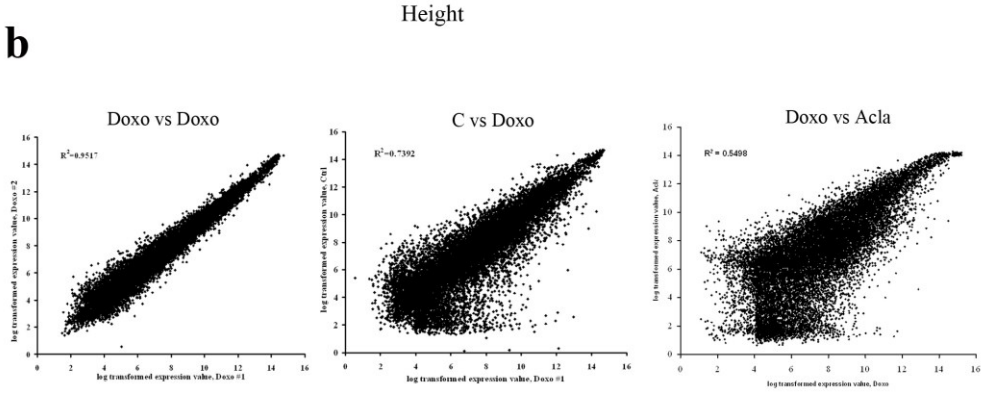

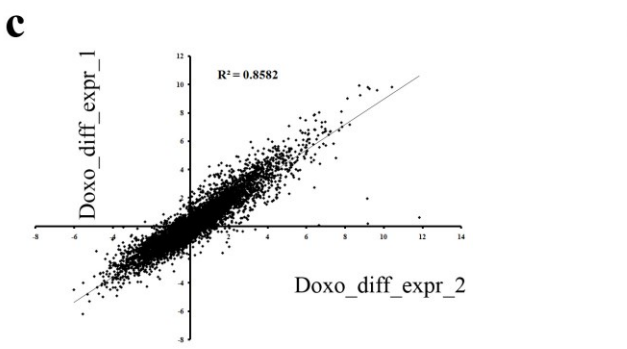

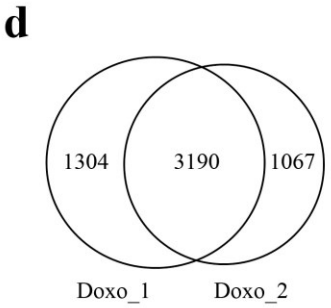

Supplementary Figure S16: Transcriptome alterations in response to different TopoII inhibitors. (**a**) Hierarchical clustering was performed on global transcription profiles (from the microarray studies in Figure 4a) determined for different cell lines exposed to the tested drugs for 2 hrs. This was followed by different periods of culturing, as indicated. Clustering was calculated using R programming. The different drugs yielded different transcription profiles. The transcriptome was affected in the similar way for cells exposed to the same drug but analyzed at different time points of culture post-drug removal. (**b**) Two independent microarray experiments of MelJuSo cells exposed to Doxo for 2 hrs followed by a 24 hr culture were performed. Gene expression levels of two independent microarray experiments were plotted for the indicated conditions and coefficients of correlation R^2 are shown in graphs. Correlations of Doxo to control cells and Doxo to Acla treatment were plotted using the identical protocol. Doxo altered the transcriptome in a consistent manner while the different drugs had different effects on the transcriptome. (**c**) Two independent experiments were performed and the fold changes (log2 transformed) of transcripts in MelJuSo cells 24 hrs post-Doxo treatment compared to the respective non-treated cells are shown in a 2D plot. Plotted are genes detected in both experiments and no fold change cut-off was applied in the plot. Note that Doxo up and down-regulated genes were consistent in the replicate experiments. (**d**) The genes altered by a factor 2 or more due to Doxo exposure (from Supplementary Figure S14c) in the duplicate experiments were compared and results expressed in a Venn diagram. 70-75% of genes differentially expressed after Doxo exposure are shared in the replicate experiments.

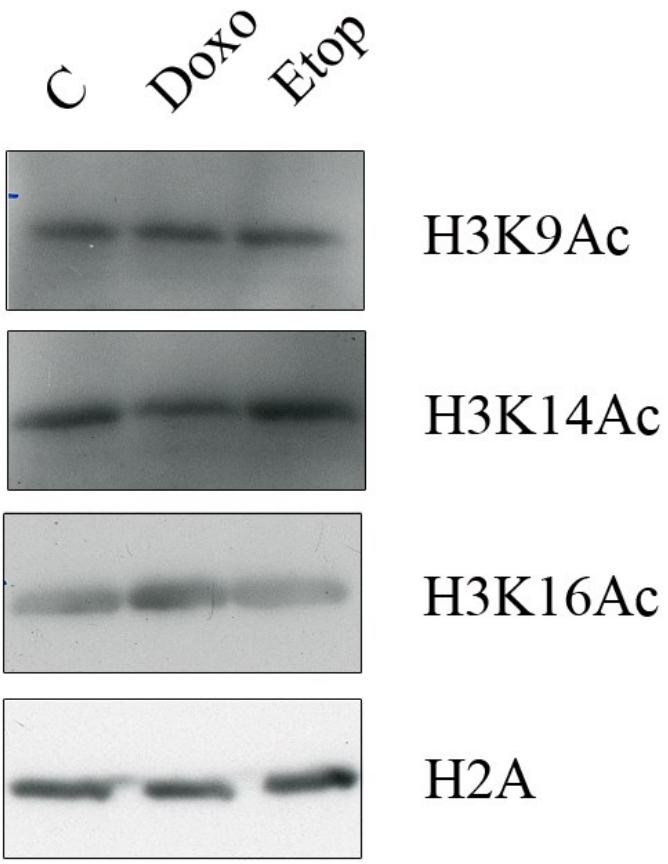

Supplementary Figure S17: Acetylated histones in chromatin after doxorubicin or etoposide exposure (relates to Figure 4b). MelJuSo cells were exposed to 9µM Doxo or 60µM Etop for 4 hrs. Chromatin was isolated, separated by SDS-PAGE and subjected to Western blot analysis with respective antibodies against modified histones and H2A, as indicated.

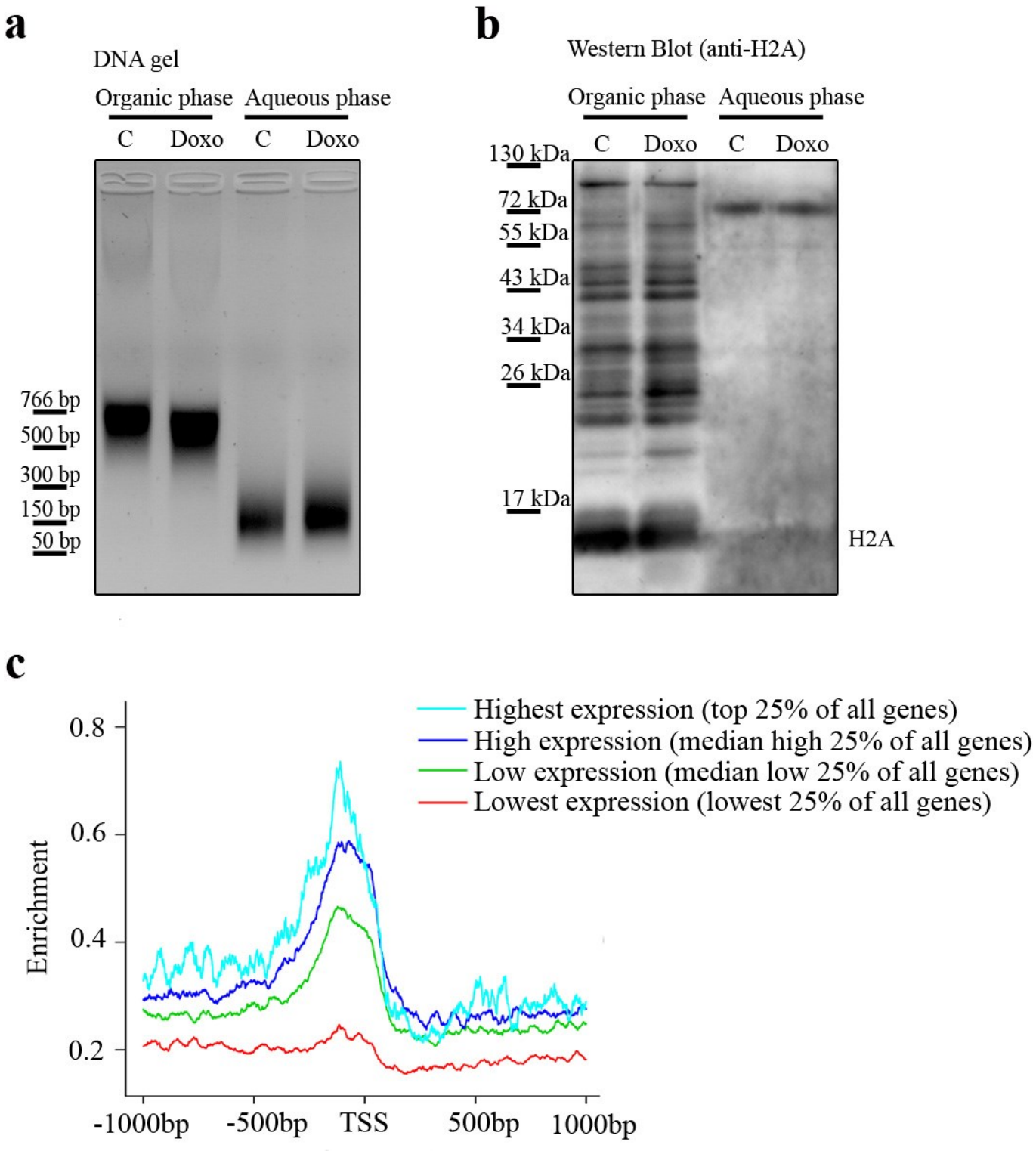

Supplementary Figure S18: The aqueous phase in FAIRE accumulates protein-free DNA. The aqueous and organic phases of the FAIRE samples of control or 9µM Doxo-exposed MelJuSo cells were subjected to DNA agarose gel electrophoreses (**a**) or SDS-PAGE followed by Western blotting analysis with anti-H2A antibodies (**b**). Same amount of input DNA was loaded on a DNA agarose gel with ethidium bromide staining. The intensities of the signal confirmed the loading of equal amounts of DNA in the different lanes. The slower migrating DNA of the organic phase may be due to additional cross-linked protein species binding to the DNA fragments while free DNA in the aqueous phase migrated faster. The Western blot filter revealed that the organic phase exclusively contained H2A and other cross-linked proteins. The position of DNA and protein markers is indicated. (**c**) Genes with higher expression have more FAIRE enrichment at promoters than genes with lower expression in non-treated MelJuSo cells.

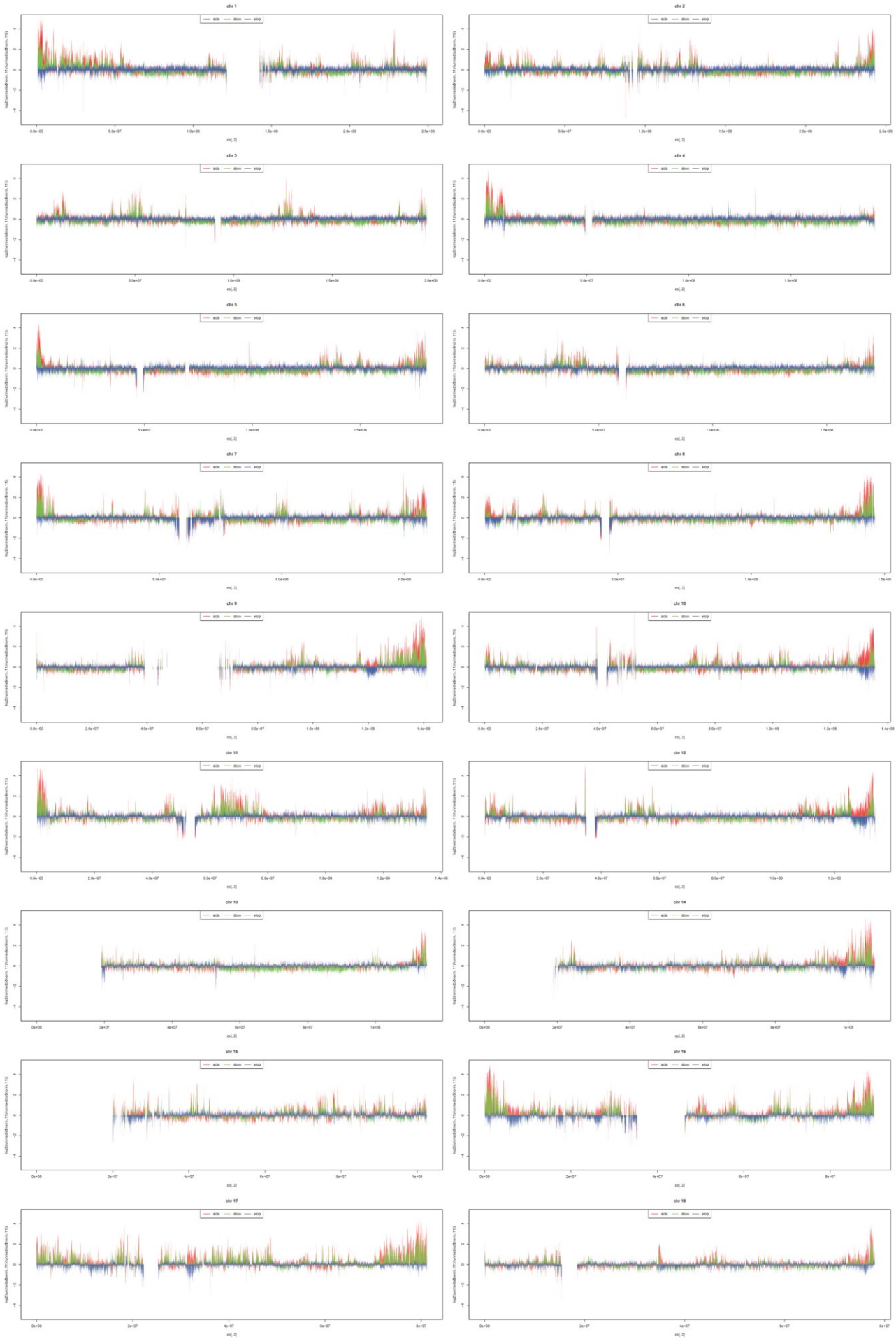
chr 1
chr 2
chr 3
chr 4
chr 5
chr 6
chr 7
chr 8
chr 9
chr 10
chr 11
chr 12
chr 13
chr 14
chr 15
chr 16
chr 17
chr 18

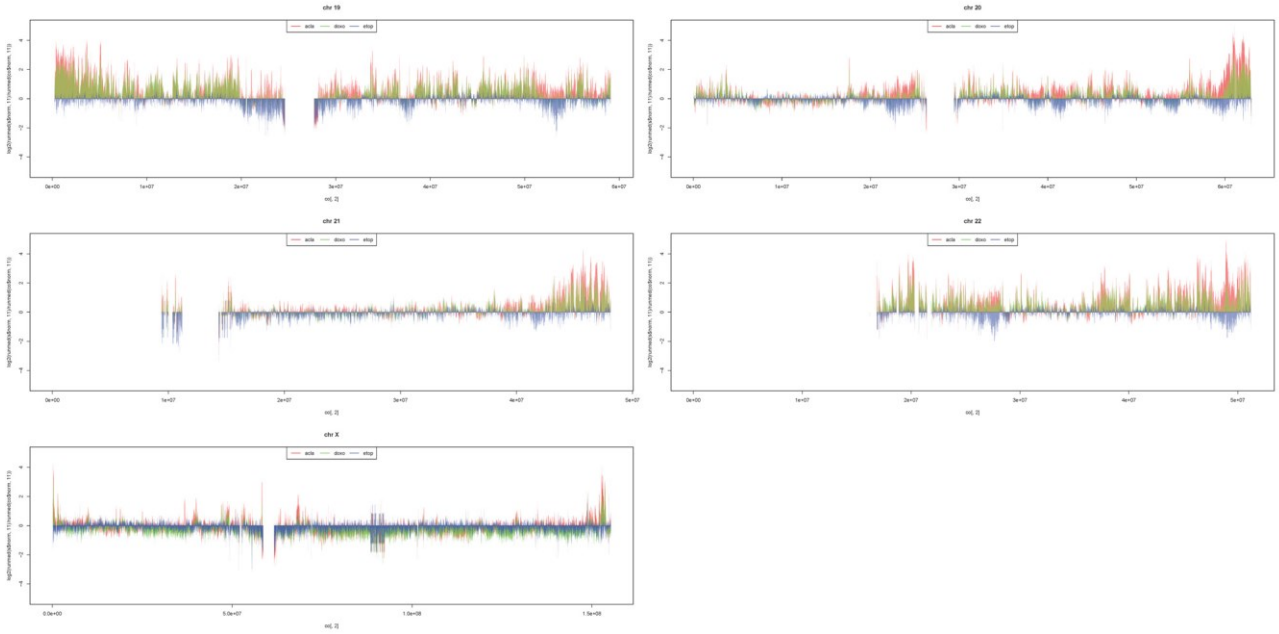

Supplementary Figure S19: Genome-wide location of histone-free DNA segments following drug exposure from MelJuSo cells (relates to Figure 4c). MelJuSo cells were cultured in the presence or absence of 9μM Doxo, 20μM Acla or 60μM Etop for 4 hrs before histone-free DNA fragments in the aqueous phase were isolated for FAIRE followed by next-generation sequencing. Shown are all chromosomes. The sequence reads (Acla, red; Doxo, green; Etop, blue) for different treatments were normalized to the same number of total uniquely mapped reads and compared to the reads of untreated MelJuSo cells. Shown is a ratio plot, as illustrated in Figure 4c for chromosome 11.

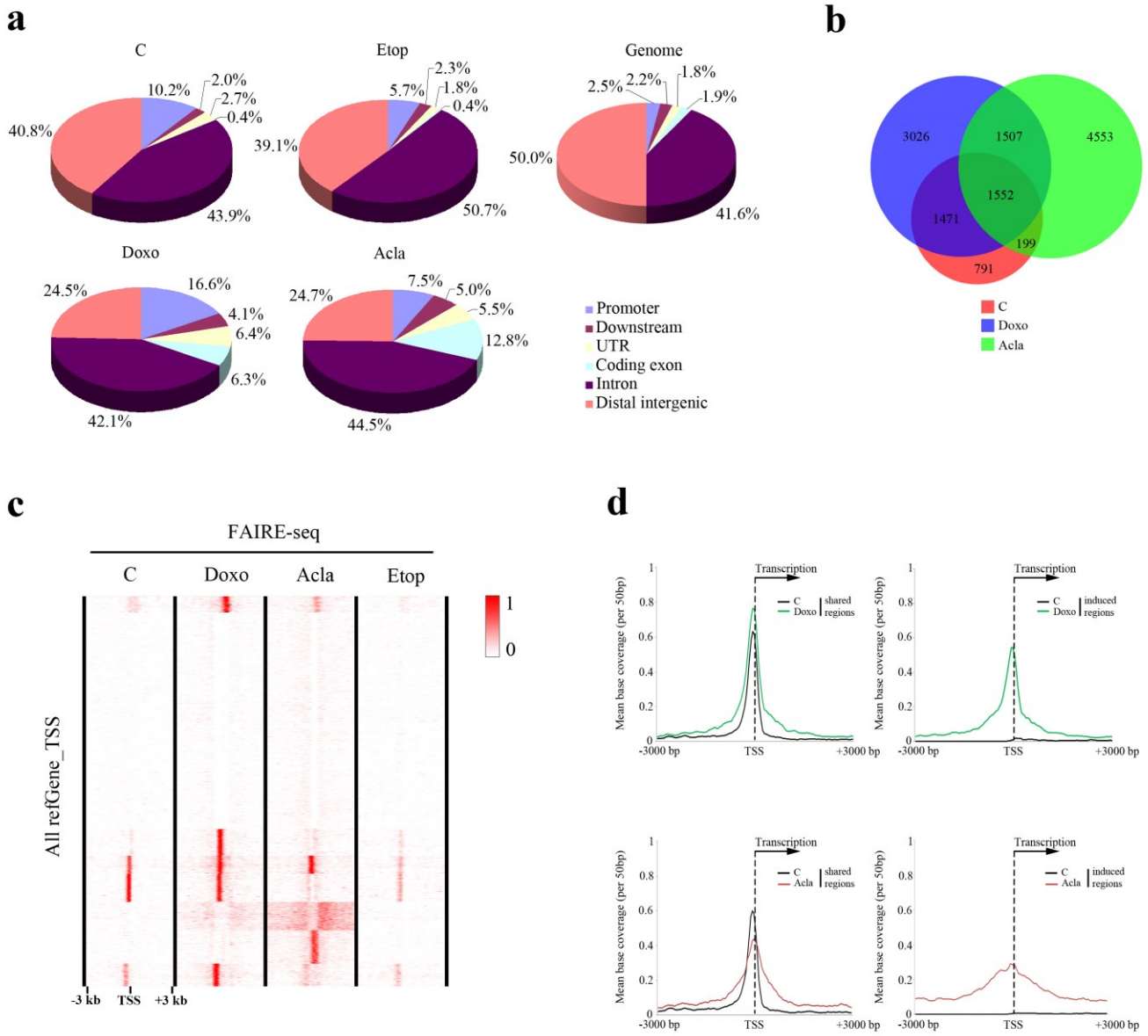

Supplementary Figure S20: Annotation of enriched histone eviction regions (relates to Figure 4d). (**a**) The peak regions were enriched to various genomic areas especially in the coding exon (light blue), promoter (blue) and UTR (yellow), in response to anthracycline treatments. Peak regions were annotated to the various genomic areas indicated using CEAS analysis. The normal distribution of the various regions in the genome is also included. (**b**) Venn diagram shows the relationship of promoter regions that have FAIRE-seq peak regions in Doxo (blue), Acla (green) or untreated (red) conditions. Promoter regions are defined as 3 kb upstream of RefSeq gene transcription starting sites. Doxo and Acla have 30-50% of altered promoter regions that are shared and 50-60% of the promoter regions that are uniquely targeted due to respective anthracycline treatment (i.e. not in control cells). (**c**) FAIRE-seq peak regions from Doxo, Acla, Etop or untreated samples were clustered around the transcription starting sites (TSS) of all RefSeq genes in a 6 kb window. Heatmap was generated using SeqMINER. Etop reduces the number of peak regions around the TSS of these genes. (**d**) FAIRE enrichment around transcription starting sites (TSS) can be sub-divided into open chromatin regions shared between non-treated and drug-treated cells (5380 of TSS for Doxo; 3319 of TSS for Acla), or drug-induced open chromatin regions (5264 of TSS for Doxo; 6712 for Acla).

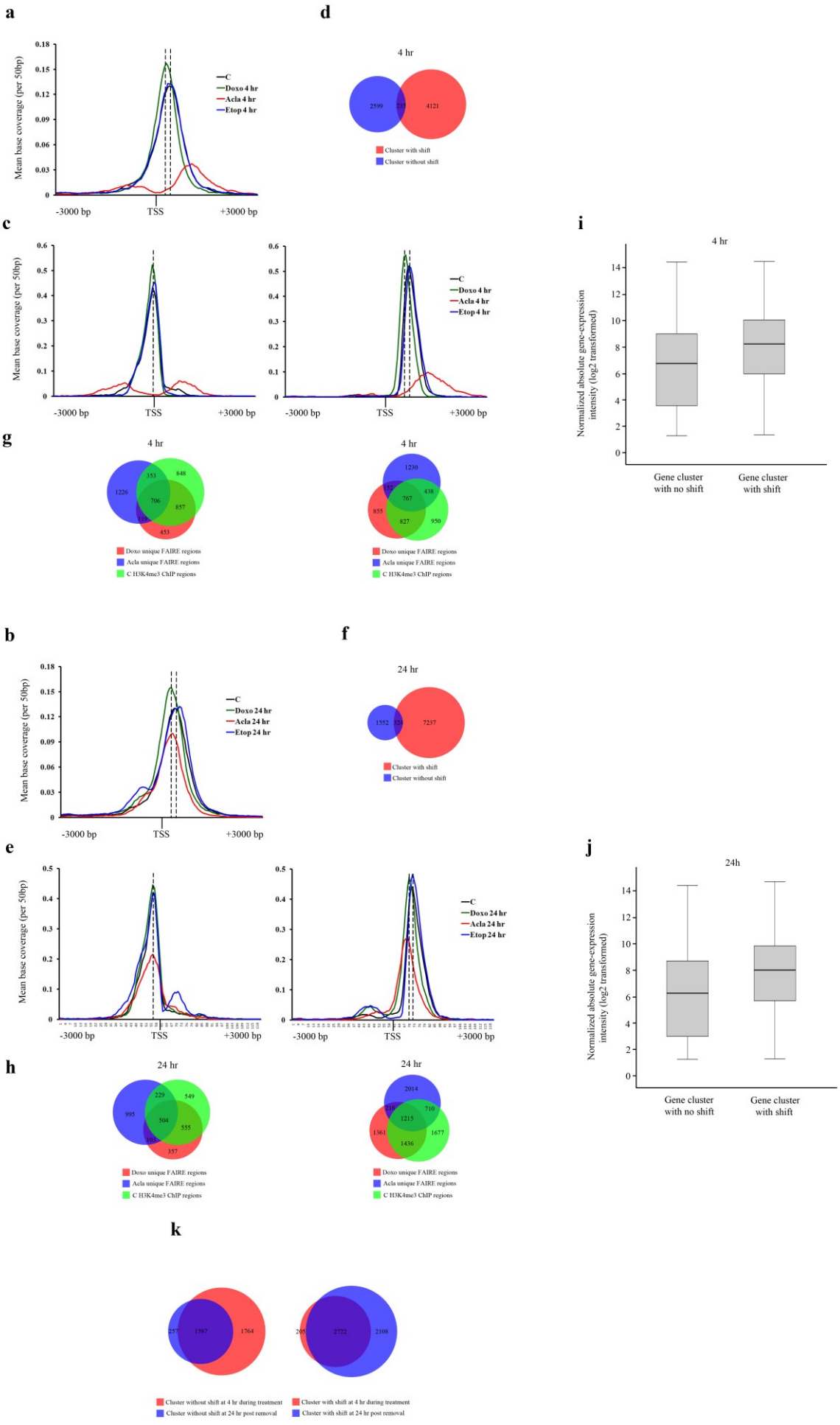
a
Mean base coverage (per 50bp)
C
Doxo 4 hr
Acla 4 hr
Etop 4 hr
-3000 bp
TSS
+3000 bp
d
4 hr
2599
234
4121
Cluster with shift
Cluster without shift
c
Mean base coverage (per 50bp)
C
Doxo 4 hr
Acla 4 hr
Etop 4 hr
-3000 bp
TSS
+3000 bp
i
4 hr
Normalized absolute gene-expression intensity (log2 transformed)
Gene cluster with no shift
Gene cluster with shift
g
4 hr
1226
353
848
706
857
453
Doxo unique FAIRE regions
Acla unique FAIRE regions
C H3K4me3 ChIP regions
4 hr
1230
438
855
767
827
950
Doxo unique FAIRE regions
Acla unique FAIRE regions
C H3K4me3 ChIP regions
b
Mean base coverage (per 50bp)
C
Doxo 24 hr
Acla 24 hr
Etop 24 hr
-3000 bp
TSS
+3000 bp
f
24 hr
1552
7237
Cluster with shift
Cluster without shift
e
Mean base coverage (per 50bp)
C
Doxo 24 hr
Acla 24 hr
Etop 24 hr
-3000 bp
TSS
+3000 bp
j
24h
Normalized absolute gene-expression intensity (log2 transformed)
Gene cluster with no shift
Gene cluster with shift
h
24 hr
995
229
549
504
555
357
Doxo unique FAIRE regions
Acla unique FAIRE regions
C H3K4me3 ChIP regions
24 hr
2014
710
1215
1361
1677
1436
Doxo unique FAIRE regions
Acla unique FAIRE regions
C H3K4me3 ChIP regions
k
1587
1764
2722
2108
Cluster without shift at 4 hr during treatment
Cluster without shift at 24 hr post removal
Cluster with shift at 4 hr during treatment
Cluster with shift at 24 hr post removal

Supplementary Figure S21: Histone H3K4me3 epigenetic marker changes position in response to anthracyclin exposure. ChIP-seq experiments were performed with anti-H3K4me3 antibody on MelJuSo cells exposed to the respective drugs either for 4 hrs or sampled 24 hrs post drug removal. Experiments were performed in independent duplicates and peak regions were called using MACS. Overlapping regions from the respective replicates were used for subsequent analyses.

Two major effects were observed for Doxo- or Acla-treated samples when compared to un-treated control or Etop-exposed samples, for peak regions aligned to TSS regions of all RefSeq genes in a 6 kb window. Whilst Acla reduced the number of peak regions (and changes location of H3K4me3 away from TSS), Doxo shifted the peaks by about 100 bp closer to TSS (as shown in panel **a** and **b**; the dotted lines indicate the peak of different curves). This effect could result from differences of histone-eviction efficiency or to additional effects imposed by the two additional sugars on Acla.
The peak regions around TSS could be subclustered into two groups: one cluster without a peak shift during Doxo treatment and another cluster with a peak shift during Doxo treatment (as shown in panel **c** and **e**; the dotted lines indicate the center of the different curves). There is no obvious relationship between these two subclusters (the shifted and non-shifted H3K4me3 peaks isolated at the same time point from MelJuSo cells), as depicted in the Venn diagrams in panel **d** and **f**. This suggests that the two regions represent defined and distinctive regions, but it was unclear what distinguishes the two different promoter regions.

To define this, we analyzed the unique FAIRE-seq peak regions from Doxo- and Acla-exposed MelJuSo cells, as well as the H3K4me3 ChIP-seq peaks in this 6 kb window, and tested whether these distinguished the two regions (panel **g** and **h**; left Venn diagrams for non-shifted and right Venn diagrams for shifted H3K4me3 peaks). No obvious differences in overlap between these two conditions and histone evicted regions were observed. This suggests that differences in chromatin structure or composition other than those tested here determine the shift of the H3K4me3 ChIP-seq peaks after Doxo exposure.
We then correlated gene expression as determined by microarray (Figure 4a) with the two subclusters (the shifted and non-shifted H3K4me3 peak regions) around the TSS. Further analysis of the genes that showed no peak shift around their TSS after Doxo exposure revealed that the expression of these genes in control cells (that is before Doxo treatment) was generally lower. The genes associated to shifted H3K4me3 peaks correlated with higher expressing genes (as shown in panel **i** for MelJuSo cells exposed to Doxo for 4 hrs, *p*-value=4.32625E-74; and panel **j** for MelJuSo cells 24 hrs after Doxo exposure, *p*-value=3.15165E-77, Fisher's exact test). This suggests that transcriptional activity of genes is sensed by Doxo. Possibly higher transcription relates to a more open structure of chromatin that may—following Doxo induced histone eviction—result in the sliding of the H3K4me3 mark. Of note, the global shift of the H3K4me3 peaks is about 100 bp, which is close to one turn of DNA around a nucleosome (147 bp).

To test whether the positions of H3K4me3 marks after Doxo exposure endured, the clusters with shifted H3K4me3 peaks from the two time points were compared. The same comparison was also performed on the clusters with non-shifted H3K4me3 peaks. This was depicted in Venn diagrams that include the numbers of the different peaks (panel **k**). A strong overlap in peak regions (defined within a 6 kb region centered at TSS) was observed between the clusters from the two time points. This suggests that Doxo alters H3K4me3 epigenetic mark of more active genes in a persistent manner. An altered cluster of H3K4me3 peaks moving away from TSS was detected 4 hrs after Acla exposure. This deviates from all other conditions (panel **a**). Yet, Acla showed similar effects as Doxo 24 hrs post drug removal (panel **b**). It could be that other epigenetic information around promoter DNA may support the recovery of this histone epigenetic mark. The molecular mechanism for this is unclear. But it is affected by the drugs with their selective effects on active genes.

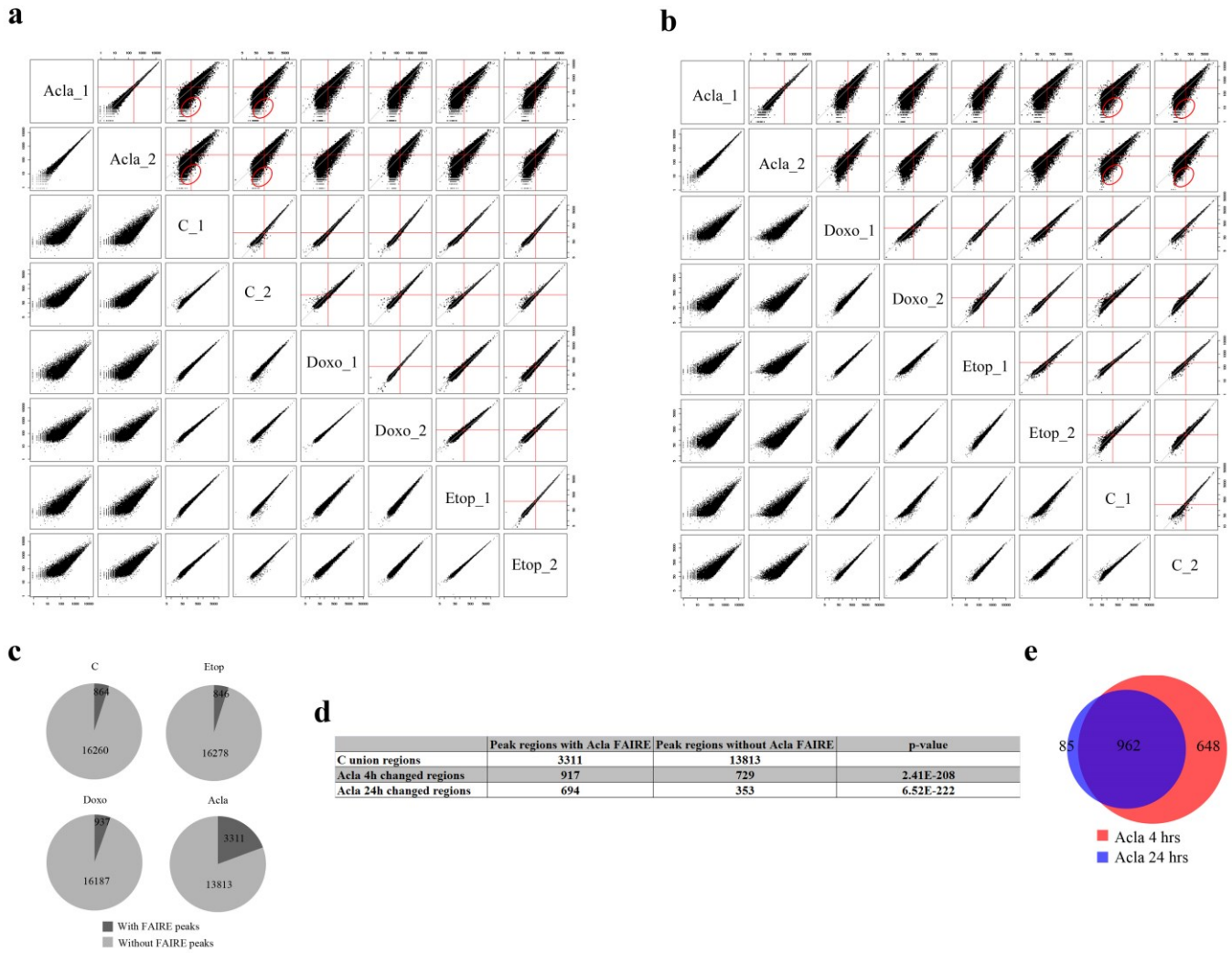

	Peak regions with Acla FAIRE	Peak regions without Acla FAIRE	p-value
C union regions	3311	13813	
Acla 4h changed regions	917	729	2.41E-208
Acla 24h changed regions	694	353	6.52E-222

Supplementary Figure S22: Histone H3K27me3 epigenetic marker changes in response to drug treatments. (**a,b**) ChIP-seq experiments were performed with anti-H3K27me3 antibody on MelJuSo cells exposed to the different drugs for 4 hrs (panel **a**) or 24 hrs post drug removal (panel **b**). Experiments were performed in duplicate. The enrichment regions were called using SICER and expressed in a 2D plot where the intensities of reads are indicated for the conditions tested. Union regions from the two control replicates were used as the window to compare the normalized read counts among all samples at different time points (as shown in panel **a** and **b**). Red lines indicate the median plus one MAD (median absolute deviation). H3K27me3 is an epigenetic marker for silenced genes and relative condensed chromatin structures. Doxo did not induce changes compared to control or Etop-exposed cells. However Acla treatment affected the peak regions of this histone modification, again illustrating a subtle difference between the two anthracyclines differing by a disaccharide only. The exact cause for this difference between Doxo and Acla is unknown. (**c**) H3K27me3 ChIP-seq union regions (without treatment) were compared to the FAIRE-seq peak regions from the MelJuSo cells treated for 4 hrs under the conditions indicated. Pie chart indicates whether the H3K27me3 ChIP-seq union regions are overlapping with FAIRE-seq regions, as an indication of possible histone-free region. Whilst H3K27me3 peaks only poorly overlapped with FAIRE-Seq peaks under control, Doxo or Etop conditions, a marked increase of FAIRE-seq peaks in H3K27me3 regions is detected in cells exposed to Acla. This again illustrates the broader effects of Acla. (**d**) H3K27me3 regions significantly affected by Acla treatment were identified comparing control and Acla replicates (as indicated in the red circle in panel a) with LIMMA package, based on 4 fold changes of the normalized reads within the same bin and a *p*-value cut-off of 0.05. The relative enrichment of Acla-induced FAIRE-seq peak regions within the H3K27me3 regions affected by Acla treatment was compared. While the Acla-induced FAIRE-seq peaks are only present in less than 25% of the H3K27me3 regions in control cells, they were strongly enriched in the H3K27me3 regions which were significantly affected in Acla-exposed cells after 4 hrs exposure or 24 hrs post-drug removal. This again illustrates an additional selectivity of Acla. (**e**) H3K27me3 regions that are significantly affected in MelJuSo cells exposed to Acla for 4 hrs or 24 hrs post drug removal (the same regions as used in panel d) were compared in a Venn diagram for overlapping locations. Acla alters a persistent set of H3K27me3 regions for a persisting period of time.

a

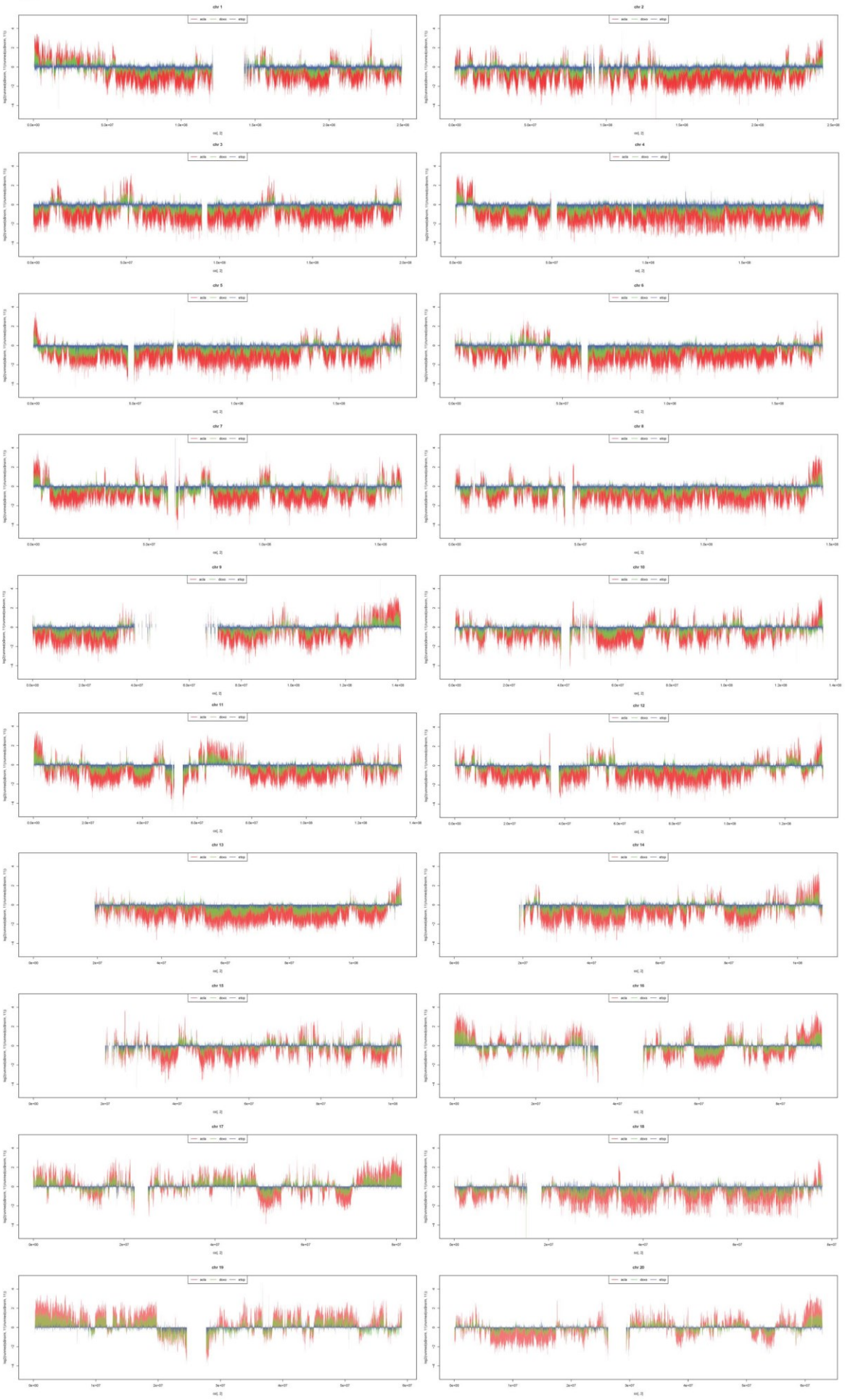
chr 1
chr 2
chr 3
chr 4
chr 5
chr 6
chr 7
chr 8
chr 9
chr 10
chr 11
chr 12
chr 13
chr 14
chr 15
chr 16
chr 17
chr 18
chr 19
chr 20

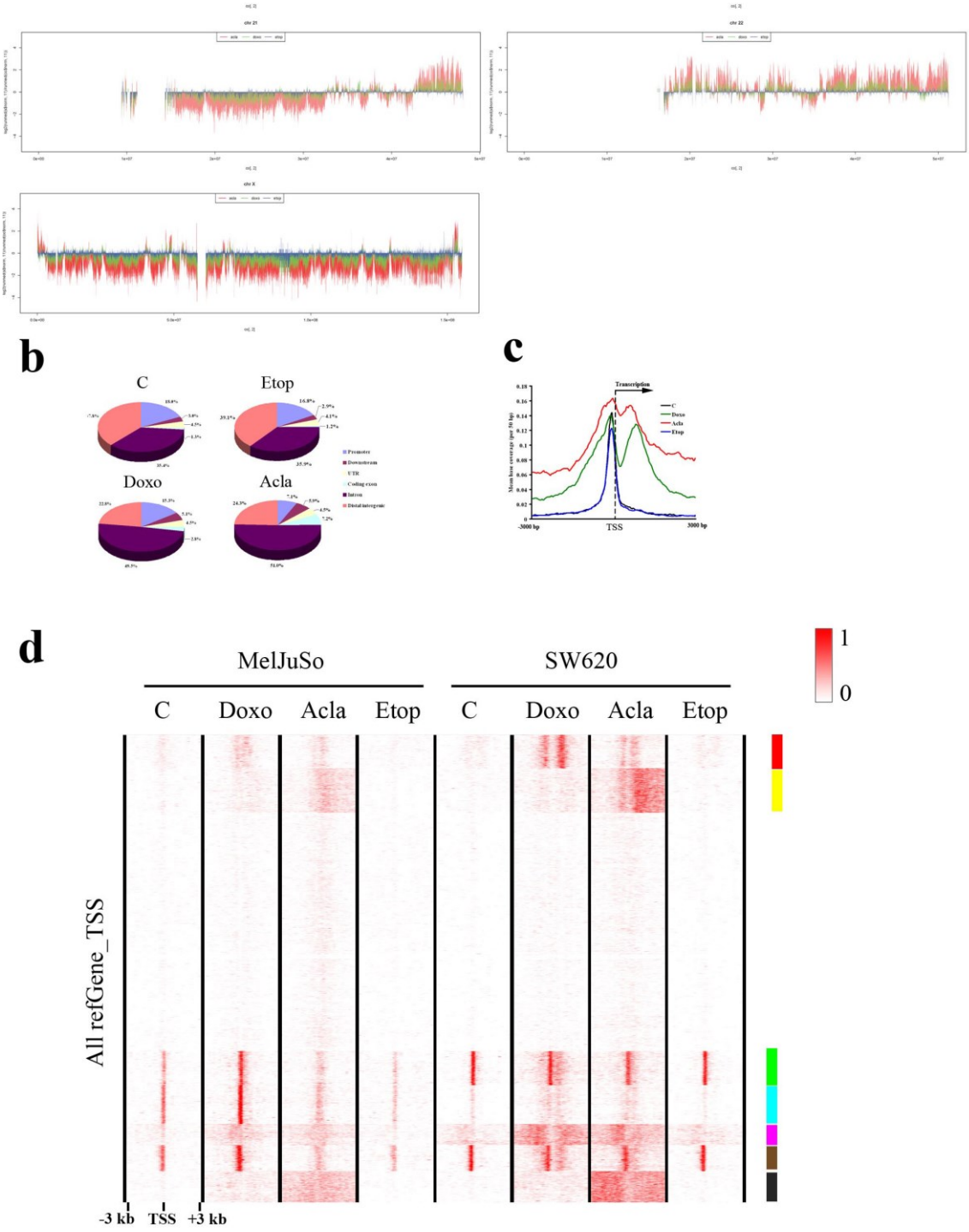

Supplementary Figure S23: Genome-wide location of histone-free DNA fragments following drug exposure of SW620 cells (relates to Figure 4c). (**a**) SW620 cells were cultured in the presence or absence of 9μM Doxo, 20μM Acla or 60μM Etop for 4 hrs before formaldehyde fixation. Histone-free DNA fragments in the aqueous phase were isolated using the FAIRE protocol followed by next generation sequencing. Shown are all chromosomes. The sequenced reads (Acla, red; Doxo, green; Etop, blue) for different treatments were normalized to the reads from untreated SW620 cells, as described for Figure 4c. Similar to MelJuSo cells, defined regions in all chromosomes are enriched for both Doxo and Acla treated samples. (**b**) Annotation of FAIRE-seq peak regions from SW620 cells, as in Supplementary Figure 18a for MelJuSo cells. Similar results for MelJuSo cells were observed, with enriched coding exons for Acla and Doxo treated samples. (**c**) Distribution of FAIRE peak regions defined in SW620 cells around TSS. The peak regions derived from FAIRE-seq were enriched for all RefSeq genes around the TSS in a 6 kb window, as in Figure 4e for MelJuSo cells. Extension of the peak regions around the TSS during Doxo or Acla treatment compared to control or Etop treated cells was also observed. (**d**) Clustering of FAIRE-seq peak regions from SW620 cells and MelJuSo cells around TSS of all RefSeq genes in a 6 kb window. Data from SW620 cells and MeJuSo cells exposed to the respective drugs as indicated were compared. Different clusters were identified, as shown in different colors at the right side of the analyses. Various clusters were affected by Doxo and Acla in both cell lines (coded red and pink), some by Acla only (coded yellow and black). There are clusters induced by Doxo which are specific for MelJuSo cells (coded blue). These results show that the effects of Doxo and Acla on chromatin are shared between cell lines. Yet Acla and Doxo are not identical in their FAIRE-seq effects and differences are also observed between the cell lines. These could relate to the differences in histone eviction by the two anthracyclines (see for example Supplementary Figure S18a and S21b) and to differences in open chromatin between cell lines.

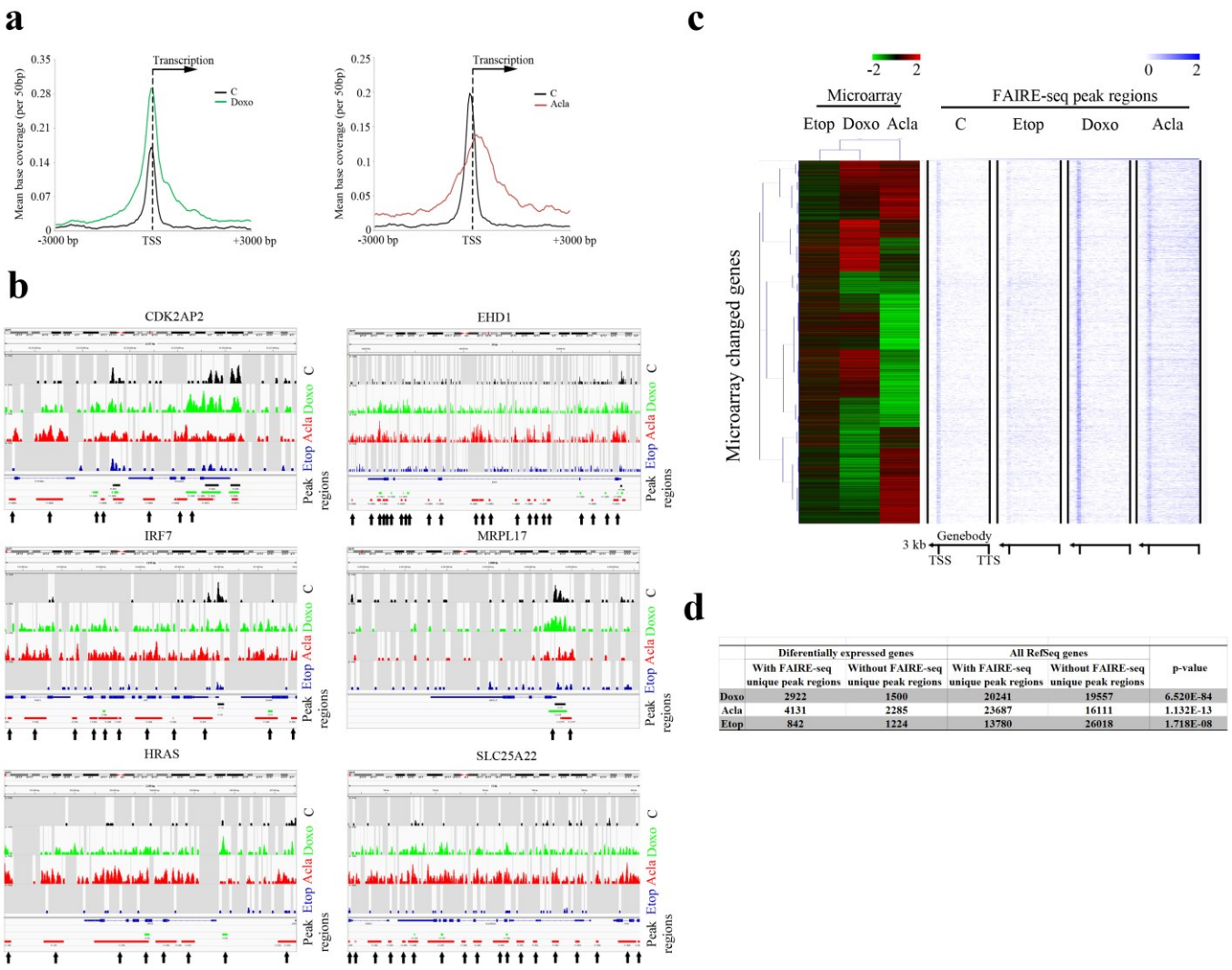

	Diferentially expressed genes		All RefSeq genes		p-value
	With FAIRE-seq unique peak regions	Without FAIRE-seq unique peak regions	With FAIRE-seq unique peak regions	Without FAIRE-seq unique peak regions	
Doxo	2922	1500	20241	19557	6.520E-84
Acla	4131	2285	23687	16111	1.132E-13
Etop	842	1224	13780	26018	1.718E-08

Supplementary Figure S24: Correlating transcriptional changes with histone eviction as detected by FAIRE-seq (relates to Figure 4f). (**a**) FAIRE enrichment around the TSS of deregulated genes exposed to Doxo (left panel) and Acla (right panel). (**b**) Examples of genes illustrating the anthracycline-induced FAIRE reads. The FAIRE-Seq reads and peak regions called for the different conditions are shown. Doxo or Acla induced unique peak regions are indicated by arrows. (**c**) Global correlation of transcription changes as detected by microarray (left panel) with the relative enrichment of FAIRE-seq peak regions in the 3 kb upstream of TSS and gene body of the corresponding genes (right panel). The color in the left panel indicates the relative fold change in microarray data of genes 24 hrs post Etop, Doxo or Acla removal as compared to untreated control cells. In the right panel, the blue color in the FAIRE-seq data indicates the base coverage of peak regions of the corresponding genes after 4 hrs drug treatment and the control situation, as indicated. Doxo and Acla affect the expression of many genes but expression can be up- or down-regulated. (**d**) Enrichment of unique FAIRE-seq peak regions on differentially expressed genes in response to different drugs. Enrichment of the unique FAIRE-seq peak regions on differentially expressed genes with the same treatment were calculated as in Figure 4f (left panel). This was compared to the enrichment of the FAIRE-seq peak regions for all RefSeq genes (right panel). *P*-values were calculated with Fisher's Exact Test. Unlike the result for Etop, unique FAIRE-seq peak regions identified in Doxo or Acla exposed cells showed a stronger correlation with the differentially expressed genes identified under identical conditions.

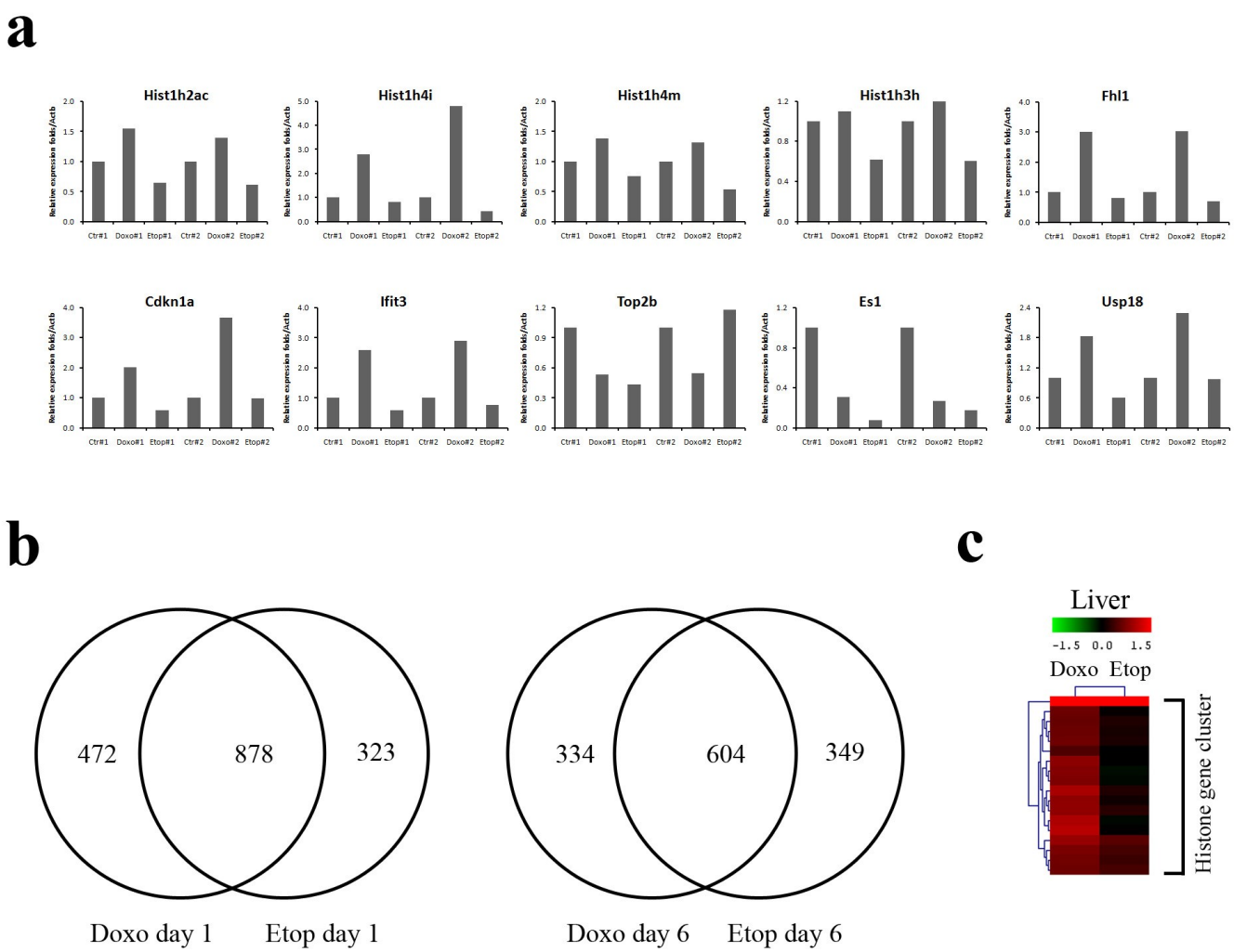

Supplementary Figure S25: Transcriptional changes in mouse organs in response to drug treatments (relates to Figure 5a). (**a**) From the microarray data of mouse heart, a set of genes were selected for qPCR validation. These genes were differentially expressed genes 1 day post Doxo treatment and contained both up- and down-regulated genes. qPCR was performed on all replicates and the results confirmed the microarray data. (**b**) Differentially expressed genes from mouse livers 1 day or 6 days after Doxo or Etop exposure were compared and expressed in Venn diagrams. About 50-70% of differentially expressed genes were shared between Doxo and Etop at the same time points. (**c**) Livers of mice bolus injected with Doxo or Etop were collected 24 hrs post injection and a part was processed for microarray analysis (the other part for histology). Heat map shows the fold change of histone gene expression in the livers of Doxo- or Etop-treated mice and is related to control mice. Color bar indicates the log-fold change compared to control.

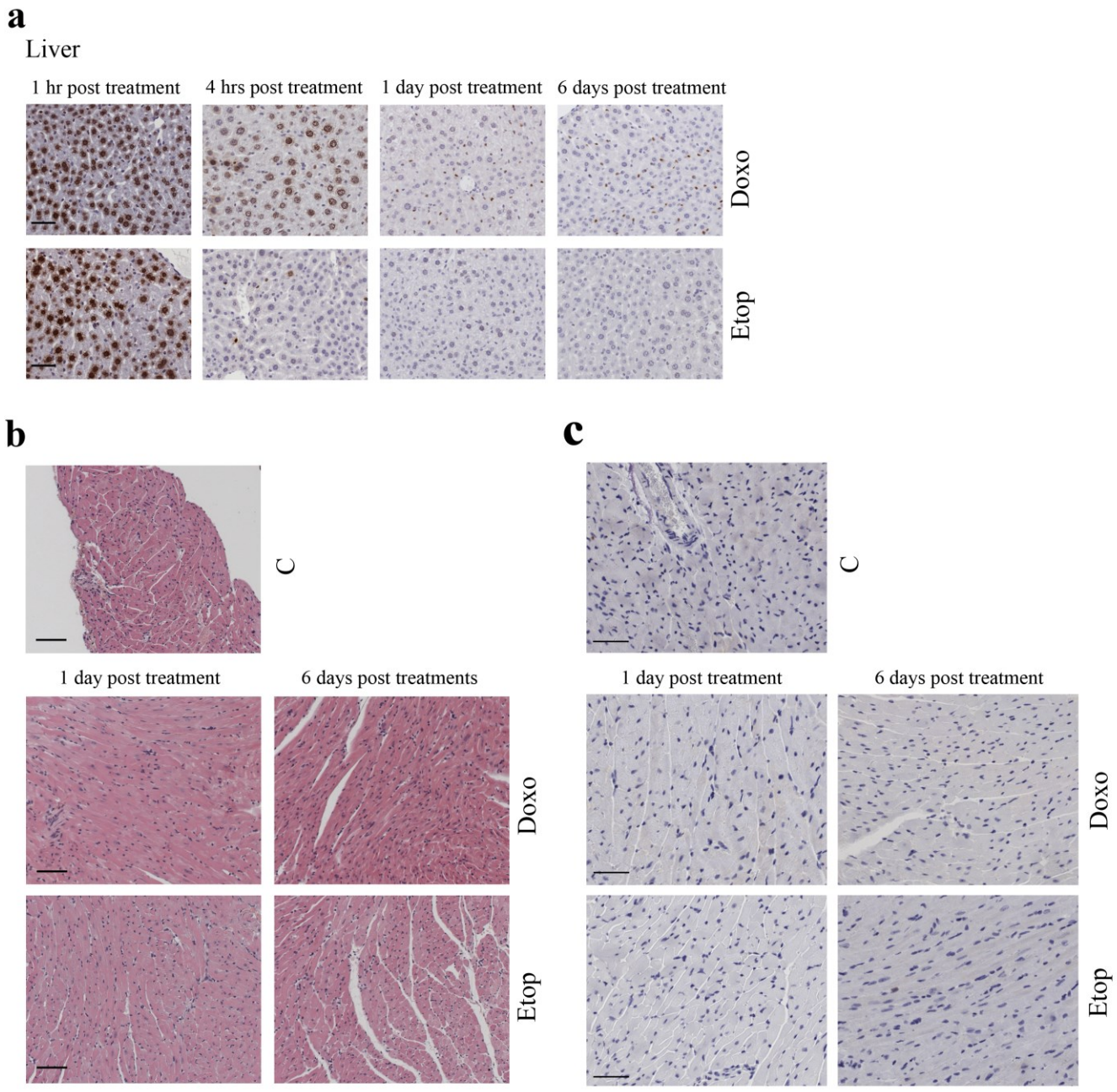

Supplementary Figure S26: Histochemical and immunohistochemical analysis of mouse tissues after acute drug treatment (relates to Figure 5). (**a**) Delayed DDR in livers of doxorubicin-treated mice. Livers of drug treated mice were collected at indicated time points for fixation and staining with anti γ-H2AX antibody. Similar results were shown for hearts with the same treatments, as in Figure 5b. Time of sampling, tissue and drug treatment is indicated. Scale bar, 50μm. (**b**) Mice received a bolus *iv* injection of Doxo or Etop and were sacrificed 1 or 6 days after injection. The same heart was divided into different parts. One part was used for microarray analysis (Figure 5a). The other part was fixed and sectioned for H&E staining and pathology analysis. Time points after injection of the respective drugs are indicated. No lymphocyte infiltration, apoptosis or necrosis was detectable by pathology analysis in all treatments. Scale bar, 20μm. (**c**) Doxorubicin does not induce cell division in mouse heart tissue. Same heart tissue samples as in Supplementary Figure 24b were stained with anti-Ki-67 antibody. No Ki-67 positive heart cells were observed. Treatment and time points of tissue isolation post-drug treatment are indicated. Induced histone gene transcription by Doxo in the heart is not due to enhanced cell division. Scale bar, 50μm.

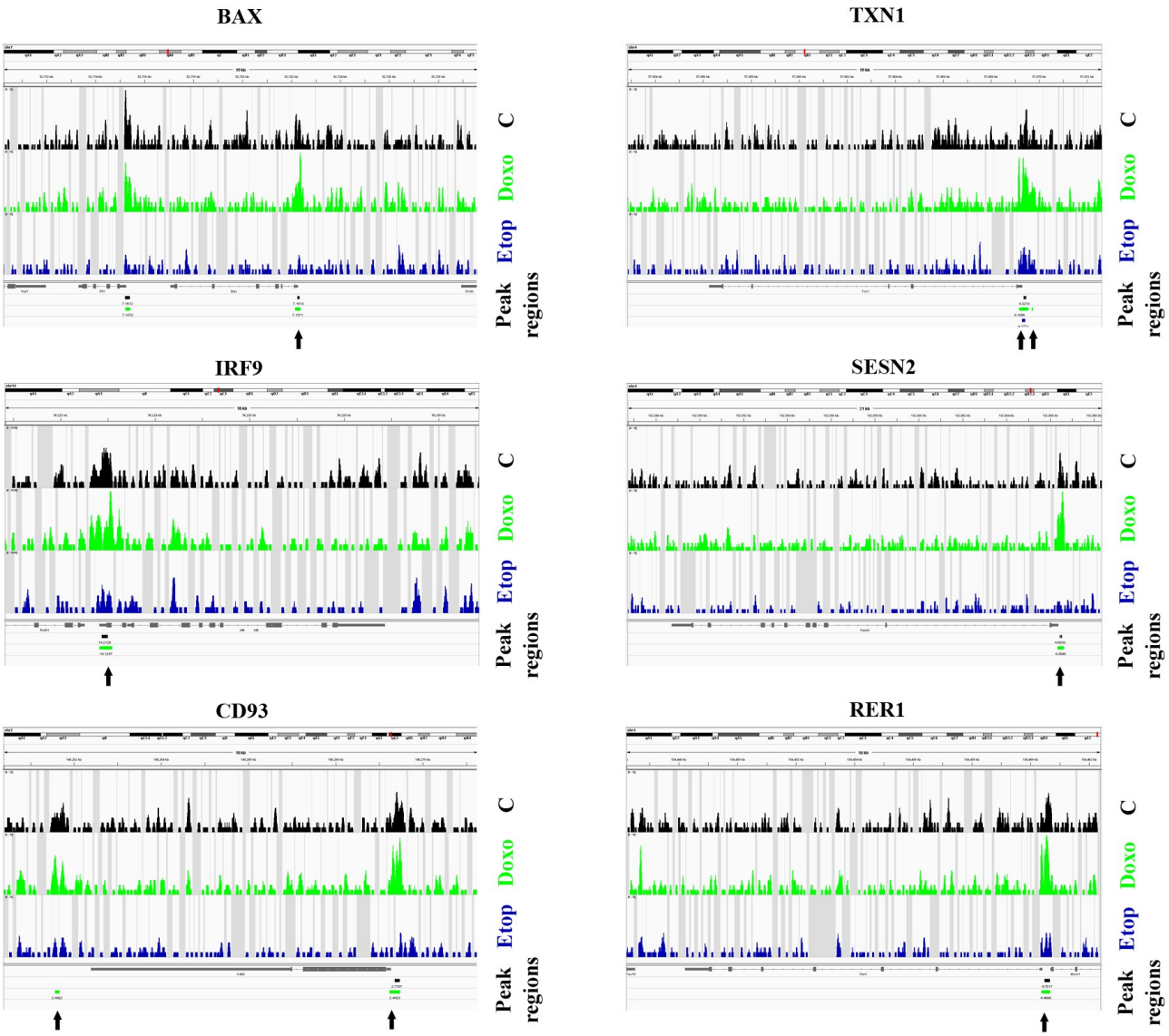

Supplementary Figure S27: Gene examples with doxorubicin-induced FAIRE regions in mouse hearts (relates to Figure 5e). The FAIRE-Seq reads and peak regions called for the different conditions are show. Doxo-induced unique peak regions are indicated by arrows.

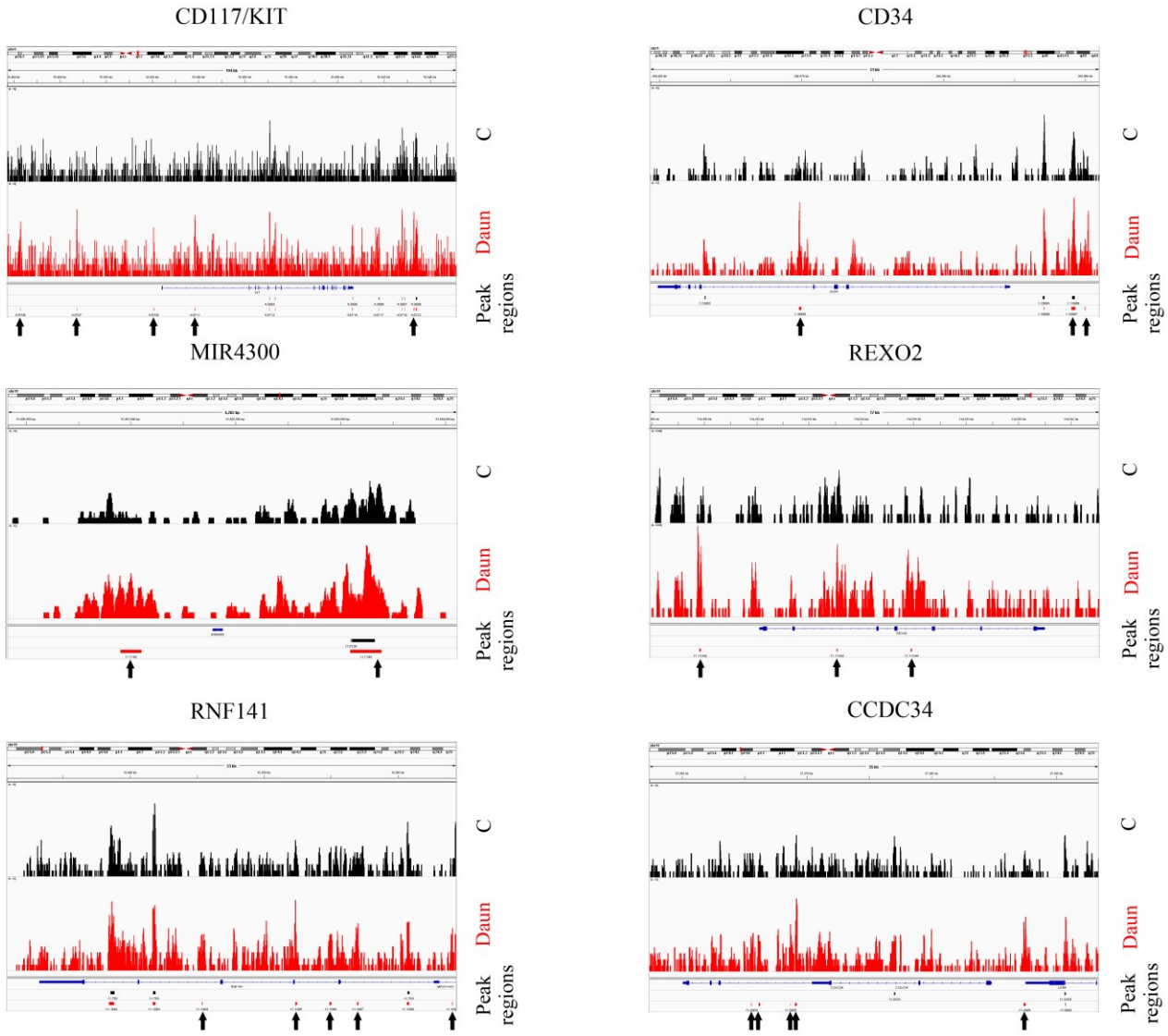

Supplementary Figure S28: Gene examples with daunorubicin-induced FAIRE regions in human AML blasts (relates to Figure 6b). The FAIRE-Seq reads and peak regions called for the different conditions are shown. Daun-induced unique peak regions are indicated by arrows.

Supplementary Table S1: List of chromatin remodeling factors and histone chaperones used for siRNA knockdown. Names of selected chromatin remodeling factors and histone chaperones that were selected for siRNA silencing are shown. DharmaFECT smart pool siRNAs targeting the respective gene were transfected in MelJuSo cells expressing PAGFP-H2A. None of these siRNAs was able to quench histone eviction following exposure to Doxo or Acla.

Official Symbol	Summary
ASF1A	**Member of the H3/H4 family of histone chaperone proteins.**
ASF1B	**Member of the H3/H4 family of histone chaperone proteins.**
CHAF1A	**Subunit of chromatin assembly factor I (CAF-I).**
CHAF1B	**Subunit of chromatin assembly factor I (CAF-I).**
CHD3	**Component of a histone deacetylase complex Mi-2/NuRD complex.**
CHD4	**Component of the nucleosome remodeling and deacetylase complex.**
INO80	**Catalytic ATPase subunit of the INO80 chromatin remodeling complex.**
NAP1L1	**Member of the nucleosome assembly protein (NAP) family.**
SMARCA2	**Member of the large ATP-dependent chromatin remodeling complex SNF/SWI.**
SMARCA4	**Member of the large ATP-dependent chromatin remodeling complex SNF/SWI.**
SMARCA5	**Component of the chromatin remodeling and spacing factor RSF.**
SSRP1	**Subunit of chromatin transcriptional elongation factor FACT.**
SUPT16H	**Subunit of chromatin transcriptional elongation factor FACT.**

Supplementary Methods

Quantitative real-time PCR

Gene expression was quantified by SYBR Green real-time PCR using the BIO-RAD Chromo4™ System (Catalog number CFB-3240). Primers were designed by PerlPrimer unless references are listed. The following primer pairs were used:

murine β-actin: 5′-GGCACCACACYTTCTACAATG-3′ (forward), 5′-GGGGTGTTGAAGGTCTCAAAC-3′ (reverse);

murine Hist1h2ac: 5′-GGCTGCTCCGCAAGGGT-3′ (forward), 5′- CTTGTTGAGCTCCTCGTCGTT-3′ (reverse)[64];

murine Hist1h4i: 5′-CAAAGCCATCTGCTTCGTCT-3′ (forward), 5′-ATGTTGTCCCGAAGCACTT-3′ (reverse)[65];

murine Hist1h4m: 5′-GAGCAGTACAGTTTTGTCTTCATC-3′ (forward), 5′-CGTGATGCCCTGGATGTTAT-3′ (reverse)[65];

murine Hist1h3h: 5′-CGCAGGACTTCAAGACCGAC-3′ (forward), 5′-GCATGATGGTGACACGCTTGG-3′ (reverse);

murine Fhl1: 5′-TACTGCGTGGATTGCTACAAGAAC-3′ (forward), 5′-GAGCCTTTACCAAACCCAGTGAT-3′ (reverse);

murine Cdkn1a: 5′-CAGACATTCAGAGCCACAGGCA-3′ (forward), 5′-GAGACAACGGCACACTTTGCTC-3′ (reverse);

murine Ifit3: 5′-CACCATCATGAGTGAGGTCAACCG-3′ (forward), 5′-TTCGACCTGGTTGCACACCCT-3′ (reverse);

murine Top2b: 5′-TGCGAAGAAAGTGAAGAAACGGA-3′ (forward), 5′-ACTTAGGTCTTTCAGCAGCTGCTC-3′ (reverse);

murine Es1: 5′-CAGACGGTTGAGGGTGATCATGG-3′ (forward), 5′-CCCATTAGGGTTCCCATTTCGAG-3′ (reverse);

murine Usp18: 5′-CTCACATGTTTGTTGGGTCACCTG-3′ (forward), 5′-CGTGTAAACCAAGAGATAGGCCGT-3′ (reverse).

Supplementary References

61 Kuijl, C. *et al.* Intracellular bacterial growth is controlled by a kinase network around PKB/AKT1. *Nature* **450**, 725-730 (2007).

62 Cook, Adam J. L., Gurard-Levin, Zachary A., Vassias, I. & Almouzni, G. A Specific Function for the Histone Chaperone NASP to Fine-Tune a Reservoir of Soluble H3-H4 in the Histone Supply Chain. *Molecular Cell* **44**, 918-927 (2011).

63 Reits, E. A. J., Benham, A. M., Plougastel, B., Neefjes, J. & Trowsdale, J. Dynamics of proteasome distribution in living cells. *EMBO J* **16**, 6087-6094 (1997).

64 Nishida, H., Suzuki, T., Ookawa, H., Tomaru, Y. & Hayashizaki, Y. Comparative analysis of expression of histone H2a genes in mouse. *BMC Genomics* **6**, 108 (2005).

65 Liu, L.-J. *et al.* Functional coupling of transcription factor HiNF-P and histone H4 gene expression during pre- and post-natal mouse development. *Gene* **483**, 1-10 (2011).